Reversions mask the contribution of adaptive evolution in microbiomes

Paul A. Torrillo [1,2] and Tami D. Lieberman [1,2,3,4+]

[1] Institute for Medical Engineering and Sciences, Massachusetts Institute of Technology, Cambridge, MA 02139, USA
[2] Department of Civil and Environmental Engineering, Massachusetts Institute of Technology, Cambridge, MA 02139, USA
[3] Broad Institute of MIT and Harvard, Cambridge, MA 02139, USA
[4] Ragon Institute of MGH, MIT, and Harvard, Cambridge, MA 02139, USA

+ Please address correspondence to tami@mit.edu

Abstract

When examining bacterial genomes for evidence of past selection, the results obtained depend heavily on the mutational distance between chosen genomes. Even within a bacterial species, genomes separated by larger mutational distances exhibit stronger evidence of purifying selection as assessed by d_N/d_S, the normalized ratio of nonsynonymous to synonymous mutations. This dependence on mutational distance, and thus time, has been proposed to arise from the inefficiency of purifying selection at removing weakly deleterious mutations. Here, we revisit this assumption in light of abundant genomes from gut microbiomes and show that a model of weak purifying selection that fits the data leads to problematic mutation accumulation. We propose an alternative model to explain the timescale dependence of d_N/d_S, in which constantly changing environmental pressures select for revertants of previously adaptive mutations. Reversions that sweep within-host populations are nearly guaranteed in microbiomes due to large population sizes, short generation times, and variable environments. Using analytical and simulation approaches, we fit the adaptive reversion model to d_N/d_S decay curves and obtain estimates of local adaptation that are realistic in the context of bacterial genomes. These results argue for interpreting low values of d_N/d_S with caution, as they may emerge even when adaptive sweeps are frequent. This work reframes an old observation in bacterial evolution, illustrates the potential of mutation reversions to shape genomic landscapes over time, and highlights the need for additional research on bacterial genomic evolution on short time scales.

Introduction

Understanding evolutionary pressures acting upon bacterial populations is crucial for predicting the emergence and future virulence of pathogens [1], modeling strategies to combat antimicrobial resistance [2], and designing genetically modified organisms [3]. Bacteria can adapt at rapid rates due to their short generation times and large population sizes. Indeed, the rapid evolutionary potential of the microbiome has been proposed to assist in dietary transitions of mammals [4]. However, the vast majority of mutations do not increase bacterial fitness, and instead result in a neutral or a deleterious effect. Thus, metrics that estimate the directionality and intensity of past selection have become critical tools in modern microbiology and biology more generally.

The normalized ratio of non-synonymous (N) to synonymous (S) substitutions, known as d_N/d_S or the K_A/K_S ratio, is a widely used indicator of past selection [5] [6] [7]. Nonsynonymous substitutions change the encoded amino acid and thus are considered likely to impact a protein's function, while synonymous substitutions do not affect the encoded amino acid and are therefore considered effectively neutral, with limited exceptions [8]. To account for the fact that nonsynonymous mutations are more likely than synonymous mutations based on the genomic code (~3X on average [9]), the values 'd_N' and 'd_S' normalize mutation counts to available sites on the genome. The d_N/d_S ratio therefore summarizes past selection on a genetic sequence, which could be a whole genome, pathway, gene, functional domain, or nucleotide. A d_N/d_S ratio of greater than 1 indicates the dominance of past adaptive evolution (i.e. directional selection) while a ratio of less than 1 traditionally implies past selection against amino acid change (purifying selection).

Early sequencing work comparing bacterial genomes of the same species reported relatively low d_N/d_S values across the whole genome (<0.15)[10] [11]. These observations, obtained from comparing distant bacteria within each species, indicated a strong predominance of purifying selection. However, as it became economically feasible to sequence organisms separated by fewer mutations and therefore less evolutionary time, a contrasting pattern emerged in which high d_N/d_S values (~1) were found between closely related strains [12] [13]. Recent work in the human microbiome has confirmed such results, and furthered the contrast between timescales by finding values of d_N/d_S greater than 1 [14][15][16]. The time scale dependence of d_N/d_S has been mainly attributed to the ongoing action of purifying selection, a model first proposed by Rocha et al. [17]. According to this model, weak purifying selection allows for an initially inflated d_N/d_S ratio, as deleterious mutations that will eventually be purged still remain in the population. As time progresses and purifying selection continuously operates, these deleterious mutations are eventually purged and the d_N/d_S ratio decreases. However, multiple studies have observed genome-wide values of d_N/d_S above 1 in these same microbial systems, with values substantially above 1 in key genes, which are simply unaccounted for in the purifying model [14][15][18][19][20].

Here, we revisit the purifying selection model in the context of the large within-person population sizes typical to the human microbiome and many bacterial infections (>10^{12} bacteria /

person). We use both analytical and simulation-based approaches to support a contrasting model for the timescale dependence of d_N/d_S, in which adaptive evolution predominates but is not apparent on long time scales.

Results

A model of purifying selection that fits the data reveals unrealistic parameters

Explaining the timescale dependence of d_N/d_S through an exclusively purifying selection model poses multiple challenges. Firstly, fitting observed data with purifying selection requires a preponderance of mutations with extraordinarily small effects on fitness (selective coefficients, s), which are challenging to eliminate effectively [21]. Secondly, the occurrence of an adaptive event during the extensive time required to purge weakly deleterious mutations interrupts the purification of such mutations. Lastly, neutral bottlenecking processes, such as those observed during host-to-host transmission, exacerbate the accumulation of deleterious mutations. For most of this section, we will disregard these last two complications and focus on the problem of small s. To provide clarity, we first detail the purifying selection model.

We divide mutations into three classes, the first two of which accumulate at a constant rate per unit time: synonymous mutations (S), neutral nonsynonymous mutations (N_{neut}), and nonneutral nonsynonymous mutations ($N_{nonneut}$). We then restate the timescale dependence of d_N/d_S as the observation that, in a population starting from a single WT cell, the average number of nonneutral nonsynonymous mutations per cell in the population ($N_{nonneut}$) increases and then asymptotes. The exclusive purifying selection model [14] [17] can now be written as:

$$\frac{d_N}{d_S} = \frac{N_{neut} + N_{nonneut}}{3S} \quad (1) \qquad \text{and} \qquad dN_{nonneut} = \mu_N dt - sN_{nonneut} dt \quad (2).$$

Here, μ_N is the nonneutral mutation rate per core genome per generation, s is the selective disadvantage of a nonneutral nonsynonymous mutation and t is the number of generations. The 3 in the denominator of (1) accounts for the discrepancy in the number of potential nonsynonymous and synonymous sites [9]. We solve for $N_{nonneut}$ by assuming $N_{nonneut}(t = 0) = 0$ to obtain:

$$N_{nonneut}(t) = \frac{\mu_N(1-e^{-st})}{s} \quad (3).$$

We can further simplify and combine these equations to create an equation for d_N/d_S with only two parameters. First, since d_N/d_S plateaus with time (Fig. 1a), we have $\lim_{t \to \infty} \frac{N_{neut} + N_{nonneut}}{3S} = \frac{N_{neut}}{3S} = \alpha$. Conveniently, α represents both the asymptote of d_N/d_S and

the proportion of nonsynonymous mutations that are neutral. This allows us to leave only s as the other free parameter, obtaining (SI Text 1.1):

$$\frac{d_N}{d_S} = \alpha + (1 - \alpha)\frac{1-e^{-st}}{st} \quad (4)$$

As sequence analysis is not privy to the actual number of generations, we approximate t assuming that synonymous mutations accumulate according to a molecular clock ($\mu_S = 0.25\mu$). As selection and mutation are both in units of per time, any change in μ results in a corresponding change in s. Model fits and consequences are largely dependent on the ratio of these two variables (more on this below), and thus are not sensitive to choice of μ. We use a relatively high mutation rate of 10^{-9} per base pair per generation [22] [23].

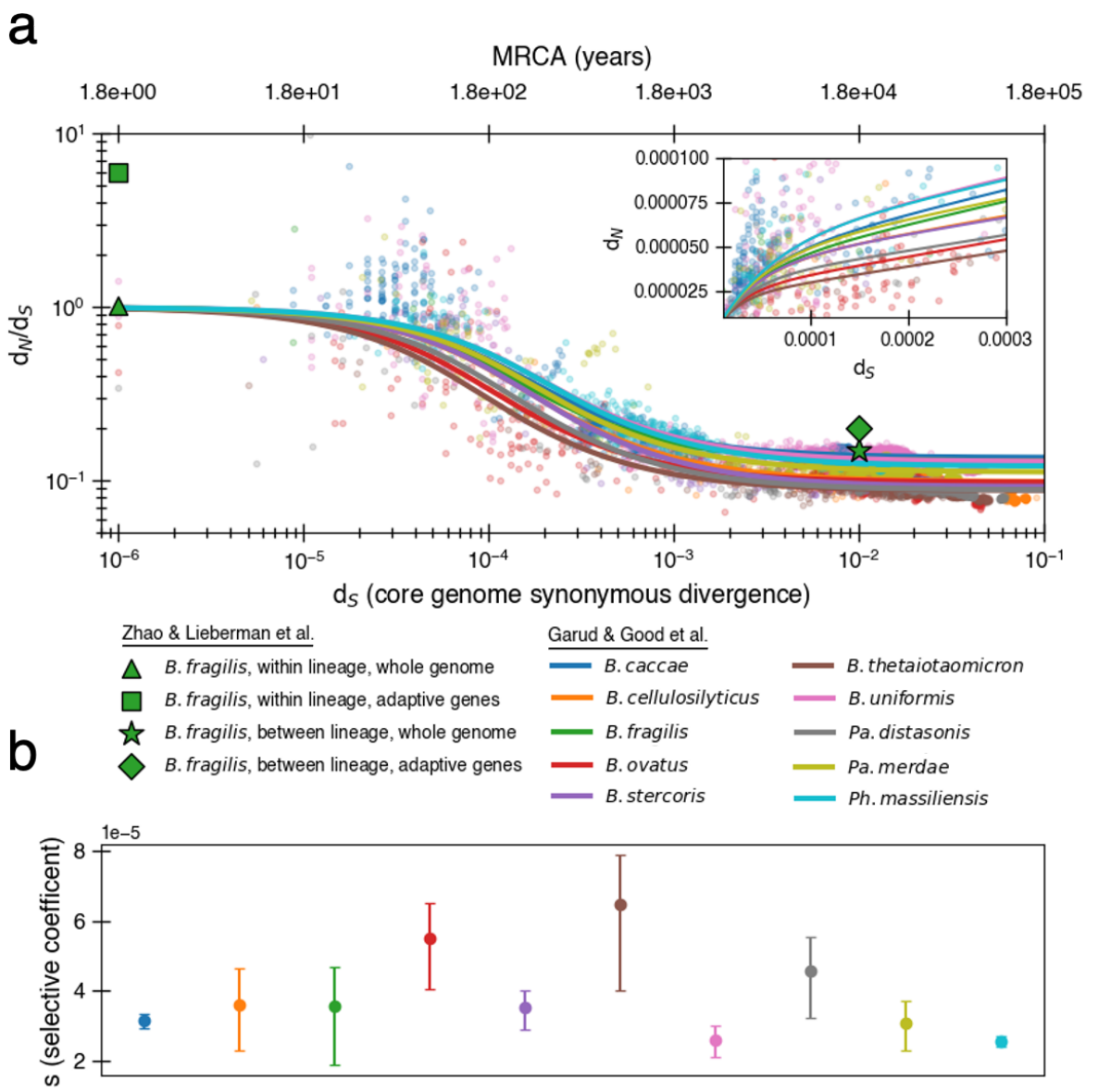

Figure 1: The canonical explanation for the time dependence of d_N/d_S is weakly purifying selection: (a) Time-dependent signature of d_N/d_S as depicted by data points derived from the studies of Garud & Good et al. [14], and Zhao & Lieberman et al. [19]. Each dot represents a pairwise comparison between the consensus sequence from two gut microbiomes as computed by [10], using only the top ten species based on quality of data points (see Methods). Fit lines were derived from these points using equation 4 to depict the trend. The median R^2 is 0.81 (range 0.54-0.94). Corresponding data from [19] confirms these observed trends, demonstrating high levels of d_N/d_S at short time scales and low levels at longer time scales. *Insets:* d_N vs d_S on linear scale. Note that the data was fit to minimize variance in the logarithmic scale not the linear scale so the fit is not expected to be as good for the inset. See Fig. S1 for the alternative. (**b**) Values of *s* from the output of 999 standard bootstrap iterations of curve fitting, conducted with replacement, demonstrate that only small values of the average selective coefficient can fit the data.

128

Fitting the data from Garud & Good et al [14], we infer median values of $\alpha \approx .10$ (0.09-0.14) and $s \approx 3.5 \times 10^{-5}$ (2.6×10^{-5}-6.5×10^{-5}) across all species (Methods, Fig. 1a). These values indicate a model in which only ~10% of nonsynonymous mutations are neutral and the remaining ~90% are so weakly deleterious that they are beyond the limit of detection of any experimental method to date [24]. Higher values of s more consistent with experimental observations [25][26][27] result in poor fits to the data (Fig. 1b; Fig. S2). However, if s is regarded as the harmonic mean of selective coefficients, a distribution of s can be constructed in which some mutations have high fitness costs more consistent with experimental data; regardless, the majority of mutations will have values of $s \sim 10^{-5}$ (SI Text 1.1).

In finite populations, the presence of so many weakly deleterious mutations becomes quickly problematic. When s is smaller than μ_N, organisms without any deleterious mutations (or with the fewest number of deleterious mutations, the "least-loaded class" [21]) can be easily lost from a finite population before they outcompete less fit organisms. The likelihood of loss depends on the population size and mutation-selection balance (μ_N/s), a parameter which estimates the average number of deleterious mutations per cell relative to the least loaded-class. Notably, the value of μ_N/s for the above fits is ~29, indicating that most cells in the population contain dozens of deleterious mutations (SI Text 1.2). We model the frequency of the least-loaded class (W), with growth proportional to its selective advantage over the total population and loss proportional to the mutation rate and obtain (SI Text 1.2):

$$W(t) = e^{-\frac{\mu_N(1-e^{-st})}{s}} \qquad (5)$$

The frequency of the least loaded class thus decreases exponentially, with decay rate proportional to μ_N/s. With $\mu_N/s = 29$, the frequency of the least-loaded class is $< 10^{-12}$ after 100,000 generations. These values were obtained conservatively assuming a core genome of 1,500,000 nucleotides (for reference the average *Bacteroides* complete genome exceeds 5,000,000 bp) that acquires deleterious mutations [14][28]; if the flexible genome also contains deleterious mutations, W is pushed down even further. Simulations substantiate this prediction of mutation accumulation and decrease in frequency of the wild type (Fig. 2a, Methods).

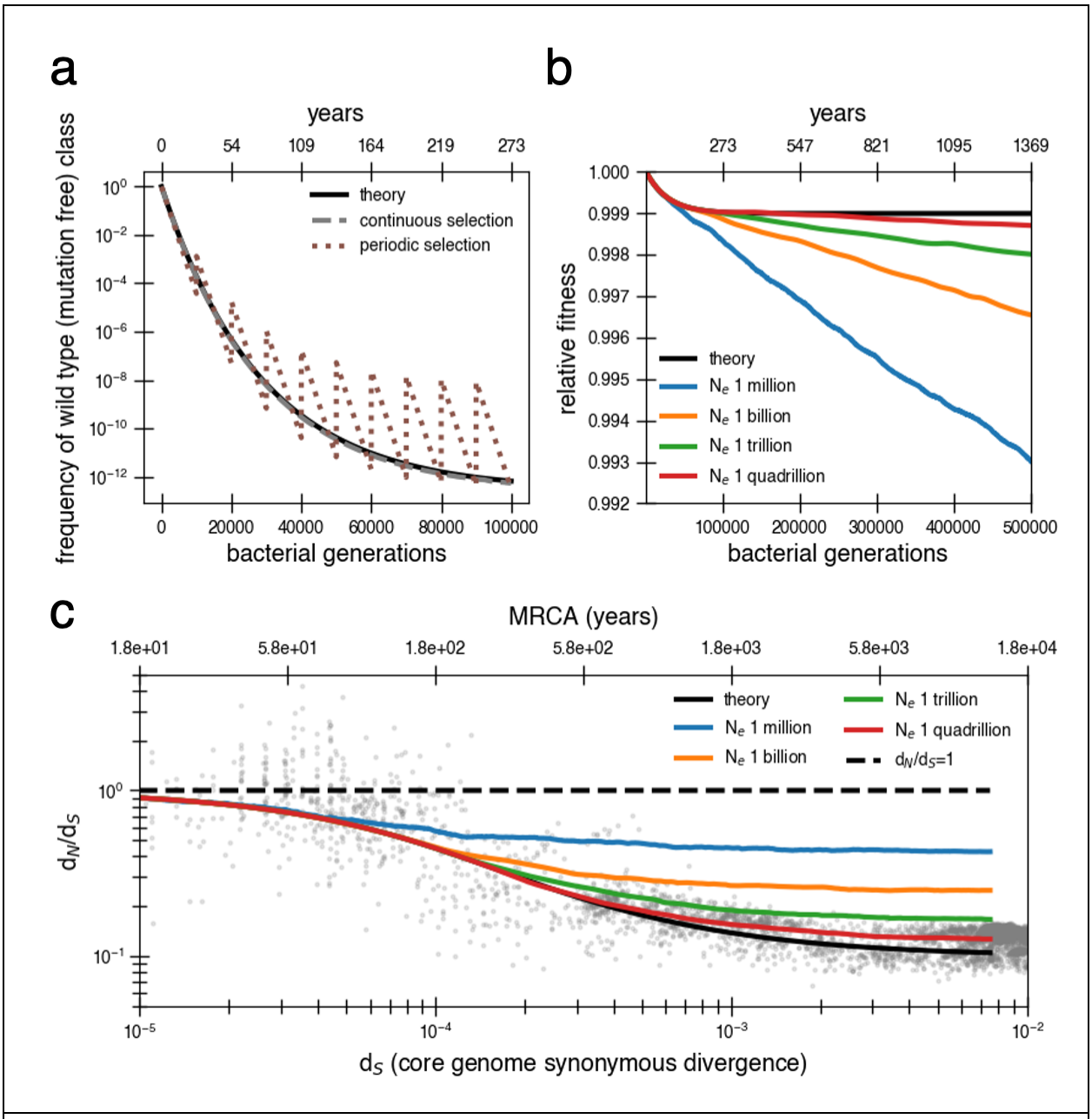

Figure 2: Models of extremely weak purifying selection that can fit the data suffer from mutation accumulation and fitness decay: (**a**) The temporal dynamics of the least-loaded class in a large population under the purifying selection model. The black line represents the predicted frequency of the wild-type (mutation-free) class over time. The "continuous selection" curve shows simulation results assuming constant purifying selection in an exceptionally large population (10^{18}) under standard assumptions. The curve "periodic selection" shows simulation results assuming selection only occurs at the time of transmission, with a significantly stronger *s* to approximate d_N/d_S decay. (**b**) As a consequence of the loss of the least-loaded class, fitness declines in finite populations over time. Colored lines indicate simulations from various effective population sizes. (**c**) Realistic global effective population sizes fail to fit the d_N/d_S curve, with different asymptotes. The black line denotes the infinite population theoretical model, while the colored lines indicate various effective population sizes. Larger values of s and models in which all mutations are deleterious cannot fit the data. (Fig. S3-S4).

The time until the least-loaded class is completely lost from the population depends on the strength of genetic drift, usually assessed using a metric called effective population size, N_e. Without extremely large effective population sizes, the least-loaded class will be lost recurrently, rapidly lowering the fitness of the population (i.e. Muller's ratchet [21][29]). Under the parameters derived above, $N_e > 10^{15}$ is required to avoid continual deleterious mutation accumulation and fitness decline (SI Text 1.2). While N_e is a complex function of census population size (estimated to be up to 10^{13} for a species in an individual gut [30] and thus 10^{23} on the globe), spatial structure, and growth dynamics, it has been estimated to range from 10^6 to 10^9 for various bacterial species considered at the global scale [31]. An N_e of 10^9 is attractive as it corresponds to almost one genotype per human host contributing to the competing global population. While higher numbers are plausible, an N_e of 10^{15} is several orders of magnitudes above the high end of previous estimates. Simulations confirm that mutation accumulation compromises the ability of the purifying model to explain empirical observations in finite populations (Fig. 2b). Moreover, continuous accumulation of mutations in such populations decreases fitness so much that the average genome contains a sizable fraction (>10%) of deleterious alleles after 1 million years (Fig. 2c, assuming $N_e = 10^9$). Even if this decreased fitness was biologically maintainable, the accumulation of so many deleterious mutations would lead to many potential adaptive back mutations, complicating the efficiency of purifying selection. Consequently, this value of μ_N/s is simply incompatible with a model where a vast majority of alleles are already optimal.

An alternative model, in which purifying selection acts only during transmission (i.e. nonsynonymous mutations are neutral in the host in which they arise) cannot prevent mutation accumulation without unrealistic assumptions. Such a model would still require ~29 non-neutral mutations in the average adult's population, while also still maintaining a least-loaded class in the global population. We consider two variants of this model. First, we simulate selection every 10,000 bacterial generations, scaling μ and s accordingly. In this model, mutations accumulate as predicted from continuous purifying selection, but only when each transmission and selection event is associated with a 30,000X increase in the frequency of the least-loaded class (Fig. 2a). Thus, this model requires hosts that are intense microbiome superspreaders. In an even more extreme model, the average host acquires all ~29 conditionally-deleterious mutations in a single human generation. Given Poisson accumulation of mutations, the frequency of the least-loaded class would dip below 10^{-12} in a single human generation-- requiring even more extreme superspreading events to be maintained. If some population exists with fewer mutations on average (e.g. children) generalists could be maintained at higher frequency. Regardless, the presence of microbiome superspreaders seems unlikely given the individual and stable nature of microbiomes at the strain level [32].

Lastly, the intolerance of the purifying model to adaptation and transmission is particularly problematic. Adaptation interferes with inefficient purifying selection; deleterious mutations are likely to hitchhike [33] to fixation on the genomic background of adaptive

mutations. Similarly, deleterious mutations also hitchhike to fixation during neutral transmission bottlenecks. These hitchhiking mutations raise the average number of deleterious mutations per cell in the population, furthering mutation accumulation and hampering the efficiency of purifying selection. Simulations confirm that adaptive sweeps have tangible impacts on d_N/d_S, including raising the asymptote (Fig. S5).

Adaptive reversions can explain the decay of d_N/d_S

If purifying selection can't explain the decay in neutral mutations, what can? One can rewrite equation (2) as a generic negative feedback model in which mutations emerge and are purged from the population at a rate proportional to how many mutations have accumulated:

$$dN_{nonneut} = R_{in}dt - P_{out}N_{nonneut}dt \quad (6).$$

In this formulation, R_{in} is simply the rate of nonneutral nonsynonymous mutation accumulation per genome per unit time and P_{out} is the loss rate of these mutations per unit time.

One particularly attractive process that could take this form is adaptive mutation and subsequent adaptive reversion of the same exact nucleotide. Reversions are likely to occur in large populations when mutations are adaptive locally but deleterious in other environments. In the gut microbiome, these alternative environments could represent different hosts (Fig. 3a). As an illustrative example, the presence of a bacteriophage in one gut microbiome might select for a loss-of-function mutation (premature stop codon or otherwise) in a phage receptor, driving this mutation to fixation within a given host. When a bacterium of this lineage later transmits to a phage-free host, it might be then adaptive to revert the receptor to its original form. Reversions are expected when compensatory mutations, those that could counteract the effects of harmful mutations, are either scarce or not as beneficial as direct reversion [34]. In particular, reversions are likely when within-host adaptation involves a premature stop codon. Notably, adaptive stop codons frequently emerge within individual people, in the context of both pathogens [1][[15][35][36] and gut commensals [19][37].

Traditionally, mutational reversions of stop codons and other mutations have been considered exceedingly unlikely and have been ignored in population genetics [38], with a few exceptions [39]. However, for a bacterial population within a human gut microbiome, the likelihood of a mutational reversion is actually quite high. A single species within the gut microbiome can have a census population size of 10^{13}, with generation rates ranging from 1-10 per day [40][41]. Taking a conservative estimate of 1 generation per day and a within-person N_e of 10^{10} (e.g. bacteria at the end of the colon may not contribute much to the next generation [42]) reversions become highly probable (Fig 3b; SI Text 2). Given a mutation rate of 10^{-9} per site per generation, we anticipate 10 mutants at any given site each generation. Consequently, if selection strongly benefits a reverting mutation (i.e. >1% selective benefit), a genotype with a beneficial mutation is essentially guaranteed to emerge within days to weeks and replace its ancestors within the host within months to years.

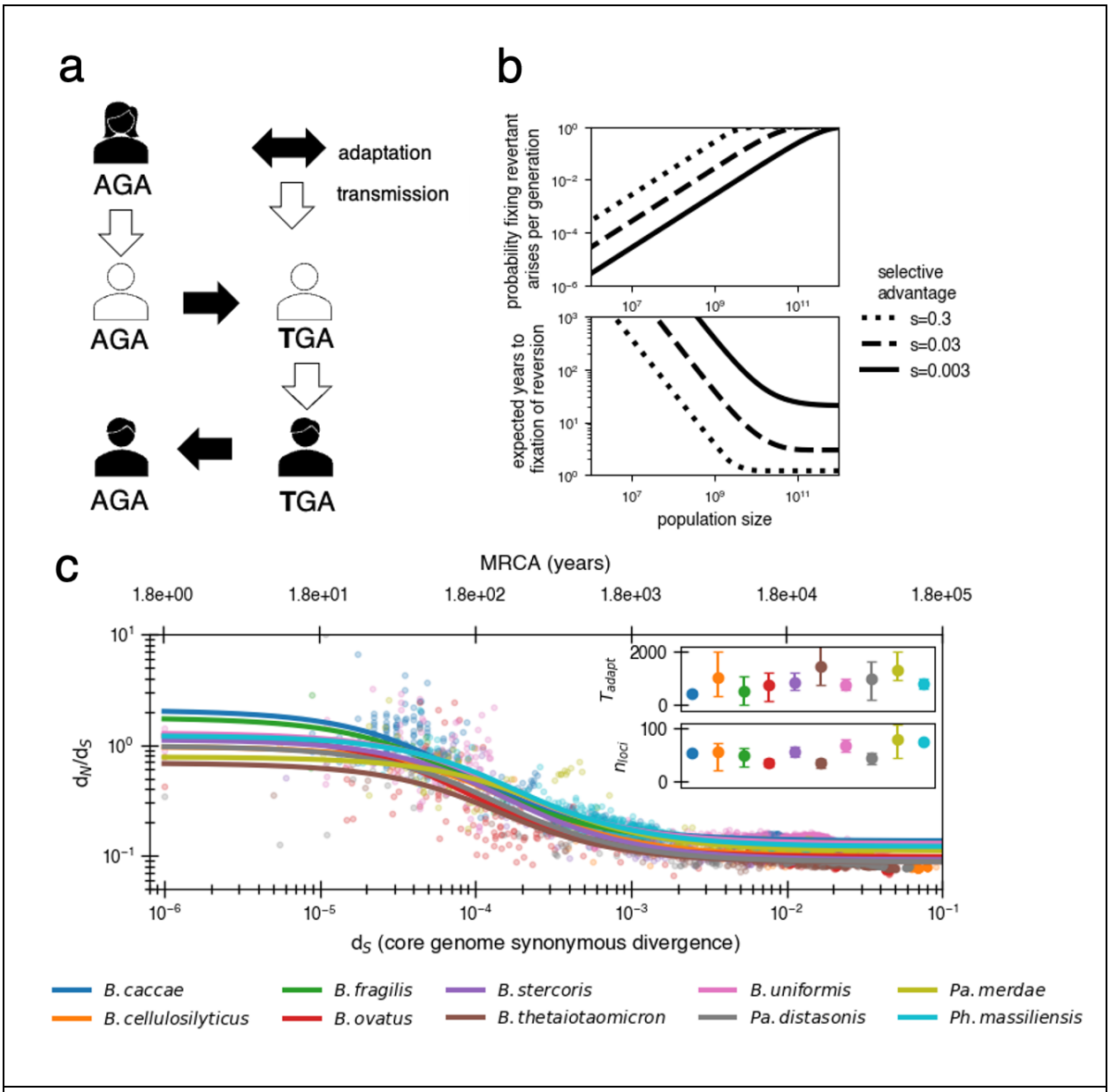

Figure 3: Locally adaptive mutations and subsequent reversions can explain the decay of nonsynonymous mutations: (**a**) Cartoon schematic depicting a potential reversion event within a single transmitted lineage of bacteria. The color of each individual indicates a different local adaptive pressure. Closed arrows represent mutation while open arrows indicate transmission. (**b**) Reversions become increasingly likely at larger population sizes, and nearly guaranteed to fix within 1-10 years when strongly beneficial in gut microbiomes. Each line type displays a different selective advantage coefficient. See SI Text 2.2 for derivation. (**c**) The adaptive reversion model can fit the data. Each colored line shows the fit for a different species. The median $r^2 = 0.82$ (range 0.54-0.94). *Insets:* Fit parameters for T_{adapt}, the average number of generations for *any* environmental pressure to switch directions and n_{loci}, the average number of sites under different fluctuating environmental pressures. The scale of the y axis is linear. Confidence intervals are from 999 bootstrapped resamples.

239

Given its plausibility, we now consider if the reversion model can explain observed decay of d_N/d_S. We incorporate fluctuating pressures into Equation (6) through a change of variables (SI text 3.1) to obtain:

$$N_{nonneut}(t) = \frac{n_{loci}}{2}\left(1 - e^{-\frac{2t}{n_{loci}T_{adapt}}}\right) \quad (7).$$

Here, n_{loci} denotes the number of distinct loci which experience fluctuating selection, and T_{adapt} represents the average number of generations required for the selective pressure on just one of these loci to change sign. We note that a locus here could be a nucleotide, gene, or gene set -- any contiguous or non-contiguous stretch of DNA in which multiple mutations interact with strong antagonism (e.g. two mutations in the same locus would be just as beneficial as only one of these). We next use equation (7) to obtain a formula for d_N/d_S that has only three free parameters when a single value for μ_S is chosen:

$$\frac{d_N}{d_S} = \alpha + \frac{n_{loci}}{6\mu_S t}\left(1 - e^{-\frac{2t}{n_{locis}T_{adapt}}}\right) \quad (8).$$

When fitting the d_N/d_S curve, the values obtained are reasonable in the context of bacterial genomics, with median best fit values across species of T_{adapt} = 840 and n_{loci} = 55. Given daily bacterial generations, this value of T_{adapt} suggests a local adaptation event approximately every two years, or less frequently if adaptive events occur in bursts (e.g. upon transmission to a new host). While 55 loci under distinct selective pressures may seem high, *Bacteroidetes* genomes are known to have dozens of invertible promoters (up to 47 in *Bacteroides fragilis* [43]). Invertible promoters are restricted out of the genome and re-ligated in the opposite direction to turn gene expression on or off. The number of invertible promoters in a given genome approximates a lower bound on the number of fluctuating selective pressures that these genomes frequently experience. Interestingly, adaptive loss-of-function mutations reported in *B. fragilis* affect the same genes regulated by invertible promoters [19]. Combining these two parameters, any given local selective force would take an average of 110 years to change sign. The plausibility of these fit parameters lends support to a model in which d_N/d_S decays solely based on strong and recurrent local adaptations.

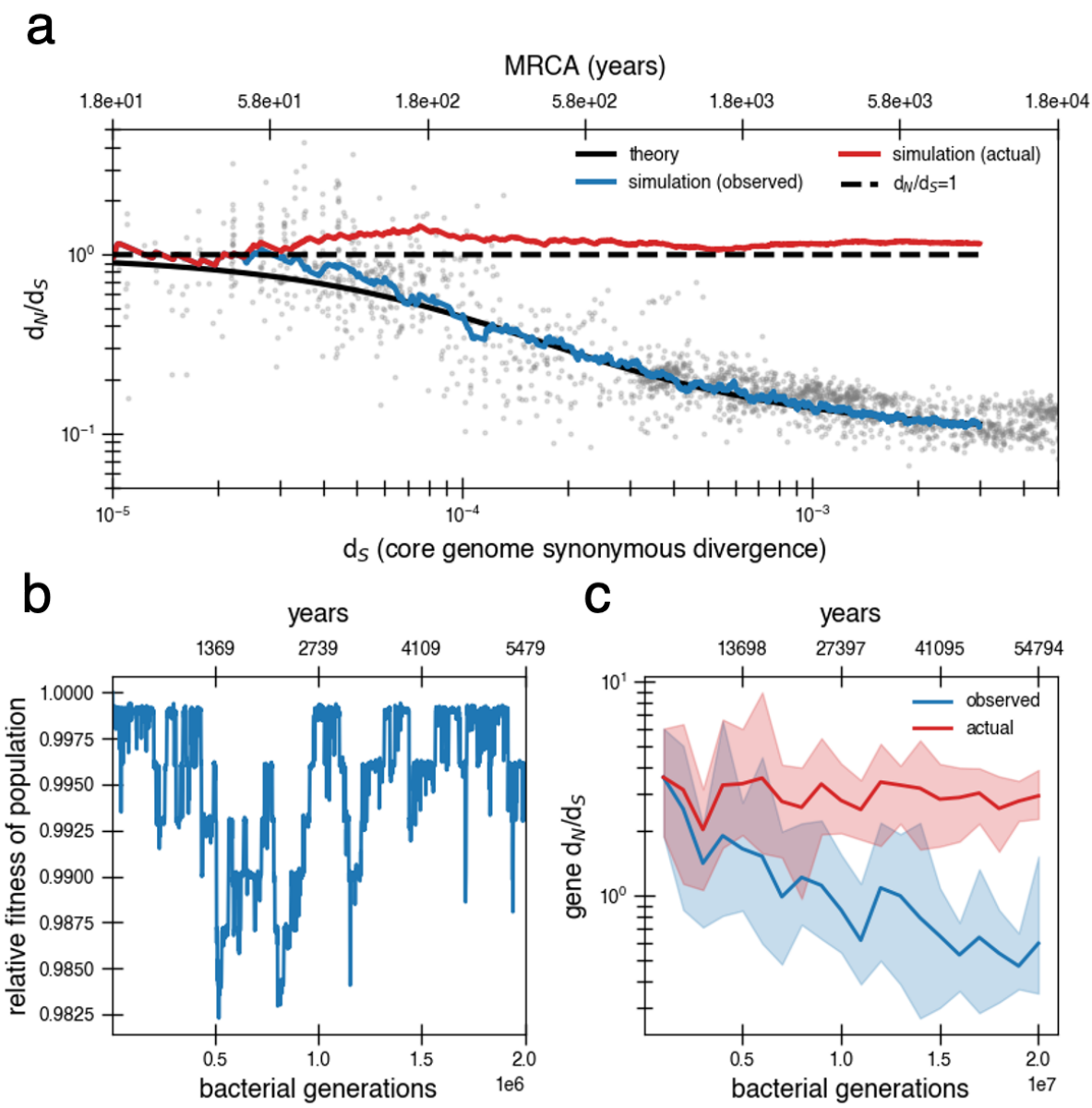

Figure 4: Under a model of reversion, the apparent d_N/d_S on long timescales underestimates the extent of adaptive evolution: (**a**) The reversion model successfully fits the data in simulations. The curve shows the average of 10 runs. We simulate a bottleneck on average every 10,000 generations (~27 years or a human generation [44]) to a population of size 1,000 from a population of 10^{10} and one beneficial mutation (s=0.03) on average every 840 generations. Each curve represents the average of 10 runs; the blue line shows the observed pairwise d_N/d_S while the red line includes adaptive mutations and reversions lost to the genomic record. (**b**) Even when discounting beneficial mutations, enabling reversion prevents fitness decay. In the simulations shown in the previous panel, deleterious mutations (s=0.003) are allowed to hitchhike, and reversions of these deleterious mutations are also permitted. Adaptive mutations and reversions are not counted in relative fitness. (**c**) PAML [45] cannot detect true d_N/d_S in a given gene in the presence of adaptive reversions. Line is the average of ten simulated phylogenies and shaded regions show the range.

To ensure a reversion model works is robust to finite populations, we performed Wright-Fisher simulations using fit parameters. These simulations capture the dynamics of single lineage evolving as it transmits across a series of hosts through random bottlenecks (Fig. 4a). As in the purifying selection model, 90% of nonsynonymous substitutions are deleterious, but this time they have a larger *s* of 0.003 [27]. Notably, while some of these deleterious mutations hitchhike to fixation during bottlenecks and adaptive sweeps, fitness does not decay because these mutations are subsequently reverted with adaptive dynamics (Fig. 4b). If deleterious mutations had a significantly smaller *s*, they would be unable to be reverted due to the long time needed to reach fixation, even if bottlenecks and adaptive events are less frequent (Fig. S5).

A critical consequence of the reversion model is that apparent and actual d_N/d_S values diverge quickly. Even when the true genome-wide d_N/d_S exceeds 1-- meaning that adaptive sweeps have been a dominant force in shaping genomes -- the observed value can be close to 0.1 on long timescales. This disparity complicates the interpretation of d_N/d_S, as it becomes challenging to determine whether a genome or gene lacks nonsynonymous mutations due to reversions or negative selection. We confirmed the inability to detect adaptive selection on a gene when reversion is rampant by simulating protein phylogenies; even the advanced software PAML [45] significantly underestimates actual d_N/d_S (Fig. 4c; Methods). Without sufficient temporal sampling, no software can realistically estimate these hidden, adaptively driven nonsynonymous mutations.

Discussion

In this study, we present a new interpretation of the time-dependent changes in d_N/d_S for bacterial populations. We show that the traditional purifying selection model struggles to replicate theoretical results in realistic population sizes, while the proposed reversion model works well. Together, these results challenge the conventional view that high d_N/d_S values over short timescales are an artifact of weak purifying selection not yet being fully realized. Moreover, the success of the reversion model suggests that adaptive dynamics can be grossly underestimated from the genomic record.

It is perhaps not surprising that reversions have been relatively overlooked in previous literature. First, most population genetics theory focuses on eukaryotic organisms with smaller population sizes and longer generation times, for which reversion is less likely. The low likelihood of reversion in these populations has inspired the use of the convenient infinite-site model [38], which assumes that reversions never occur and simplifies derivations. While smaller population sizes can be appropriate for modeling global bacterial dynamics-- because bottlenecks and geography limit how many organisms effectively compete-- they are inappropriate for within-gut populations, which are less structured. While gut microbiomes do have spatial structure that reduces competition, theoretical work modeling this biogeography suggests that the census and active population sizes differ only ~10-fold [42][46]. This brings the within-gut microbiome N_e to substantially larger than the per-nucleotide mutation rate, invalidating the

311 infinite sites model. Secondly, while bacterial geneticists have long observed adaptive
312 loss-of-function mutations, two common misinterpretations of population genetic parameters can
313 underestimate the probability of reversion: molecular clock rates (μ), which are generally low,
314 can easily be confused with the supply of potential mutations (μN_e) [47]; and classical
315 approaches that assess N_e from genetic diversity vastly underestimate the currently active
316 population size, particularly if a bottleneck recently occurred (e.g. during transmission). Lastly,
317 simulating large populations, even when appropriate, is computationally difficult. As a
318 consequence, population genetics simulations, including those of bacteria, have used relatively
319 small population sizes ($\leq 10^6$ organisms). We overcome computational limitations by tracking
320 genetic classes rather than individual genotypes (Methods).

321 Whether or not a reversion model can be applied beyond microbial populations remains
322 to be explored. When effective population sizes are smaller than 10^9, reversions are relatively
323 unlikely. For example, while reversions are likely to sweep individual gut microbiomes, we do
324 not propose that reversions sweep the global bacterial population. Regardless, theoretical work
325 on animal populations has shown that adaptive reversions are possible after population
326 bottlenecks [39]. Similarly, environmental variations that change extremely rapidly (e.g. those
327 imposed by daily dietary changes) would be less likely to drive fixation and reversion than the
328 less rapid changes considered here (e.g. phage migration) as very rapid changes would increase
329 clone competition [48]. On the other hand, adaptive reversions may be particularly relevant for
330 viral populations, which are known to undergo within-host adaptation, have very large
331 population sizes, and experience frequent bottlenecks [49]. In fact, reversions have commonly
332 been observed in certain regions of the HIV genome, and have been postulated to diminish
333 measured substitution rates in those regions [50].

334 An alternative potential model posits that local adaptation is rampant, and that only
335 generalists can transmit -- making lineages with adaptive mutations "dead ends" [1]. Such a
336 model is very similar to a model in which purifying selection acts only during transmission. As
337 we have shown, such a model requires unrealistic superspreading given that prolonged residency
338 in a specific host increases the likelihood of losing generalist traits. Though a model of exclusive
339 "dead ends" is therefore unlikely, we do not rule out the possibility that some combination of
340 irreversible and reversible local adaptations can explain the timescale dependence of d_N/d_S.

341 While we focus on point mutation reversions for their mathematical convenience, we
342 note that recombination with ancestral genotypes could drive adaptive reversions. Microbial
343 geneticists have frequently observed that recombined regions exhibit lower d_N/d_S values
344 compared to non-recombined regions [51], a signature consistent with having already
345 experienced reversion or purifying selection. Recombination could potentially revert multiple
346 mutations simultaneously, and it is therefore likely, despite the success of the mutation-driven
347 model, that recombination likely plays a role in local adaptation and reversion.

348 Adaptive reversions have not yet been observed for human gut microbes. We propose that
349 lack of evidence is simply an artifact of lacking samples along a line of descent with sufficient
350 genomic resolution. We note that adaptation and reversion would not result in parallel evolution

in the genomic record if various initial mutations result in the same phenotype (i.e. loss of function mutations). Ample evidence supports the plausibility of our reversion model. Short-term studies of bacterial evolution, including in the gut microbiome, have revealed bacterial parallel evolution [15][18][19][52], loss-of-function changes like premature stop codons [35], and low long-term d_N/d_S values in short-term pseudogenized genes [53].

The success of the reversion model calls for sample collection from new cohorts -- designed to catch real-world bacterial populations along lines of descent -- to fully establish its relevance. More broadly, our results highlight the importance of simulating large population sizes, spotlight the potential for local adaptation in bacterial populations, and underscore the need for continued population genetics work for microbial populations.

References

[1] Culyba MJ, Van Tyne D. Bacterial evolution during human infection: Adapt and live or adapt and die. PLoS Pathog. 2021 Sep 9;17(9):e1009872. doi: 10.1371/journal.ppat.1009872. PMID: 34499699; PMCID: PMC8428787.

[2] Davies J, Davies D. Origins and evolution of antibiotic resistance. Microbiol Mol Biol Rev. 2010 Sep;74(3):417-33. doi: 10.1128/MMBR.00016-10. PMID: 20805405; PMCID: PMC2937522.

[3] Castle SD, Grierson CS, Gorochowski TE. Towards an engineering theory of evolution. Nat Commun. 2021 Jun 7;12(1):3326. doi: 10.1038/s41467-021-23573-3. PMID: 34099656; PMCID: PMC8185075.

[4] Kolodny O, Schulenburg H. Microbiome-mediated plasticity directs host evolution along several distinct time scales. Philos Trans R Soc Lond B Biol Sci. 2020 Sep 28;375(1808):20190589. doi: 10.1098/rstb.2019.0589. Epub 2020 Aug 10. PMID: 32772662; PMCID: PMC7435166.

[5] Jukes TH, Cantor CR (1969). Evolution of Protein Molecules. New York: Academic Press. pp. 21–132

[6] Kryazhimskiy S, Plotkin JB. The population genetics of dN/dS. PLoS Genet. 2008 Dec;4(12):e1000304. doi: 10.1371/journal.pgen.1000304. Epub 2008 Dec 12. PMID: 19081788; PMCID: PMC2596312.

[7] Barber MF, Elde NC. Escape from bacterial iron piracy through rapid evolution of transferrin. Science. 2014 Dec 12;346(6215):1362-6. doi: 10.1126/science.1259329. PMID: 25504720; PMCID: PMC4455941.

[8] Nowick K, Walter Costa MB, Höner Zu Siederdissen C, Stadler PF. Selection Pressures on RNA Sequences and Structures. Evol Bioinform Online. 2019 Aug 29;15:1176934319871919. doi: 10.1177/1176934319871919. PMID: 31496634; PMCID: PMC6716170.

[9] Yang Z, Nielsen R. Estimating synonymous and nonsynonymous substitution rates under realistic evolutionary models. Mol Biol Evol. 2000 Jan;17(1):32-43. doi: 10.1093/oxfordjournals.molbev.a026236. PMID: 10666704.

[10] Jolley KA, Kalmusova J, Feil EJ, Gupta S, Musilek M, Kriz P, Maiden MC. Carried meningococci in the Czech Republic: a diverse recombining population. J Clin Microbiol. 2000 Dec;38(12):4492-8. doi: 10.1128/JCM.38.12.4492-4498.2000. PMID: 11101585; PMCID: PMC87626.

[11] Dingle KE, Colles FM, Wareing DR, Ure R, Fox AJ, Bolton FE, Bootsma HJ, Willems RJ, Urwin R, Maiden MC. Multilocus sequence typing system for Campylobacter jejuni. J Clin Microbiol. 2001 Jan;39(1):14-23. doi: 10.1128/JCM.39.1.14-23.2001. PMID: 11136741; PMCID: PMC87672.

[12] Feil EJ, Cooper JE, Grundmann H, Robinson DA, Enright MC, Berendt T, Peacock SJ, Smith JM, Murphy M, Spratt BG, Moore CE, Day NP. How clonal is Staphylococcus aureus? J Bacteriol. 2003 Jun;185(11):3307-16. doi: 10.1128/JB.185.11.3307-3316.2003. PMID: 12754228; PMCID: PMC155367.

[13] Baker L, Brown T, Maiden MC, Drobniewski F. Silent nucleotide polymorphisms and a phylogeny for Mycobacterium tuberculosis. Emerg Infect Dis. 2004 Sep;10(9):1568-77. doi: 10.3201/eid1009.040046. PMID: 15498158; PMCID: PMC3320301.
[14] Garud NR, Good BH, Hallatschek O, Pollard KS. Evolutionary dynamics of bacteria in the gut microbiome within and across hosts. PLoS Biol. 2019 Jan 23;17(1):e3000102. doi: 10.1371/journal.pbio.3000102. PMID: 30673701; PMCID: PMC6361464.
[15] Lieberman TD, Michel JB, Aingaran M, Potter-Bynoe G, Roux D, Davis MR Jr, Skurnik D, Leiby N, LiPuma JJ, Goldberg JB, McAdam AJ, Priebe GP, Kishony R. Parallel bacterial evolution within multiple patients identifies candidate pathogenicity genes. Nat Genet. 2011 Nov 13;43(12):1275-80. doi: 10.1038/ng.997. PMID: 22081229; PMCID: PMC3245322.
[16] Shoemaker WR, Chen D, Garud NR. Comparative Population Genetics in the Human Gut Microbiome. Genome Biol Evol. 2022 Jan 4;14(1):evab116. doi: 10.1093/gbe/evab116. PMID: 34028530; PMCID: PMC8743038.
[17] Rocha EP, Smith JM, Hurst LD, Holden MT, Cooper JE, Smith NH, Feil EJ. Comparisons of dN/dS are time dependent for closely related bacterial genomes. J Theor Biol. 2006 Mar 21;239(2):226-35. doi: 10.1016/j.jtbi.2005.08.037. Epub 2005 Oct 18. PMID: 16239014.
[18] Marvig RL, Sommer LM, Molin S, Johansen HK. Convergent evolution and adaptation of Pseudomonas aeruginosa within patients with cystic fibrosis. Nat Genet. 2015 Jan;47(1):57-64. doi: 10.1038/ng.3148. Epub 2014 Nov 17. PMID: 25401299.
[19] Zhao S, Lieberman TD, Poyet M, Kauffman KM, Gibbons SM, Groussin M, Xavier RJ, Alm EJ. Adaptive Evolution within Gut Microbiomes of Healthy People. Cell Host Microbe. 2019 May 8;25(5):656-667.e8. doi: 10.1016/j.chom.2019.03.007. Epub 2019 Apr 23. PMID: 31028005; PMCID: PMC6749991.
[20] Zhao S, Dai CL, Evans ED, Lu Z, Alm EJ. Tracking strains predicts personal microbiomes and reveals recent adaptive evolution. bioRxiv 2020 Sep; doi: 10.1101
[21] Haigh J. The accumulation of deleterious genes in a population--Muller's Ratchet. Theor Popul Biol. 1978 Oct;14(2):251-67. doi: 10.1016/0040-5809(78)90027-8. PMID: 746491.
[22] Drake JW, A constant rate of spontaneous mutation in DNA-based microbes. Proc Natl Acad Sci USA 88, 7160–7164 (1991).
[23] Barrick JE, Lenski RE. Genome dynamics during experimental evolution. Nat Rev Genet. 2013 Dec;14(12):827-39. doi: 10.1038/nrg3564. Epub 2013 Oct 29. PMID: 24166031; PMCID: PMC4239992.
[24] Gallet R, Cooper TF, Elena SF, Lenormand T. Measuring selection coefficients below 10(-3): method, questions, and prospects. Genetics. 2012 Jan;190(1):175-86. doi: 10.1534/genetics.111.133454. Epub 2011 Oct 31. PMID: 22042578; PMCID: PMC3249376.
[25] Kibota TT, Lynch M. Estimate of the genomic mutation rate deleterious to overall fitness in E. coli. Nature. 1996 Jun 20;381(6584):694-6. doi: 10.1038/381694a0. PMID: 8649513.
[26] Trindade S, Perfeito L, Gordo I. Rate and effects of spontaneous mutations that affect fitness in mutator Escherichia coli. Philos Trans R Soc Lond B Biol Sci. 2010 Apr 27;365(1544):1177-86. doi: 10.1098/rstb.2009.0287. PMID: 20308092; PMCID: PMC2871818.

[27] Robert L, Ollion J, Robert J, Song X, Matic I, Elez M. Mutation dynamics and fitness effects followed in single cells. Science. 2018 Mar 16;359(6381):1283-1286. doi: 10.1126/science.aan0797. PMID: 29590079.
[28] Nayfach S, Pollard KS. Average genome size estimation improves comparative metagenomics and sheds light on the functional ecology of the human microbiome. Genome Biol. 2015 Mar 25;16(1):51. doi: 10.1186/s13059-015-0611-7. PMID: 25853934; PMCID: PMC4389708.
[29] Neher RA, Shraiman BI. Fluctuations of fitness distributions and the rate of Muller's ratchet. Genetics. 2012 Aug;191(4):1283-93. doi: 10.1534/genetics.112.141325. Epub 2012 May 29. PMID: 22649084; PMCID: PMC3416007.
[30] Sender R, Fuchs S, Milo R. Revised Estimates for the Number of Human and Bacteria Cells in the Body. PLoS Biol. 2016 Aug 19;14(8):e1002533. doi: 10.1371/journal.pbio.1002533. PMID: 27541692; PMCID: PMC4991899.
[31] Bobay LM, Ochman H. Factors driving effective population size and pan-genome evolution in bacteria. BMC Evol Biol. 2018 Oct 12;18(1):153. doi: 10.1186/s12862-018-1272-4. PMID: 30314447; PMCID: PMC6186134.
[32] Faith JJ, Guruge JL, Charbonneau M, Subramanian S, Seedorf H, Goodman AL, Clemente JC, Knight R, Heath AC, Leibel RL, Rosenbaum M, Gordon JI. The long-term stability of the human gut microbiota. Science. 2013 Jul 5;341(6141):1237439. doi: 10.1126/science.1237439. PMID: 23828941; PMCID: PMC3791589.
[33] Desai MM, Walczak AM, Fisher DS. Genetic diversity and the structure of genealogies in rapidly adapting populations. Genetics. 2013 Feb;193(2):565-85. doi: 10.1534/genetics.112.147157. Epub 2012 Dec 5. PMID: 23222656; PMCID: PMC3567745.
[34] Levin BR, Perrot V, Walker N. Compensatory mutations, antibiotic resistance and the population genetics of adaptive evolution in bacteria. Genetics. 2000 Mar;154(3):985-97. doi: 10.1093/genetics/154.3.985. PMID: 10757748; PMCID: PMC1460977.
[35] Key FM, Khadka VD, Romo-González C, Blake KJ, Deng L, Lynn TC, Lee JC, Chiu IM, García-Romero MT, Lieberman TD. On-person adaptive evolution of Staphylococcus aureus during treatment for atopic dermatitis. Cell Host Microbe. 2023 Apr 12;31(4):593-603.e7. doi: 10.1016/j.chom.2023.03.009. PMID: 37054679; PMCID: PMC10263175.
[36] Shopsin B, Drlica-Wagner A, Mathema B, Adhikari RP, Kreiswirth BN, Novick RP. Prevalence of agr dysfunction among colonizing Staphylococcus aureus strains. J Infect Dis. 2008 Oct 15;198(8):1171-4. doi: 10.1086/592051. PMID: 18752431
[37] Barreto HC, Sousa A, Gordo I. The Landscape of Adaptive Evolution of a Gut Commensal Bacteria in Aging Mice, Current Biology, Volume 30, Issue 6,2020, Pages 1102-1109.e5, ISSN 0960-9822, https://doi.org/10.1016/j.cub.2020.01.037.
[38] Tajima, F. Infinite-allele model and infinite-site model in population genetics. *J. Genet.* 75, 27–31 (1996). https://doi.org/10.1007/BF02931749

[39] Charlesworth J, Eyre-Walker A. The other side of the nearly neutral theory, evidence of slightly advantageous back-mutations. Proc Natl Acad Sci U S A. 2007 Oct 23;104(43):16992-7. doi: 10.1073/pnas.0705456104. Epub 2007 Oct 16. PMID: 17940029; PMCID: PMC2040392

[40] Korem T, Zeevi D, Suez J, Weinberger A, Avnit-Sagi T, Pompan-Lotan M, Matot E, Jona G, Harmelin A, Cohen N, Sirota-Madi A, Thaiss CA, Pevsner-Fischer M, Sorek R, Xavier R, Elinav E, Segal E. Growth dynamics of gut microbiota in health and disease inferred from single metagenomic samples. Science. 2015 Sep 4;349(6252):1101-1106. doi: 10.1126/science.aac4812. Epub 2015 Jul 30. PMID: 26229116; PMCID: PMC5087275.

[41] Sender R, Fuchs S, Milo R. Revised Estimates for the Number of Human and Bacteria Cells in the Body. PLoS Biol. 2016 Aug 19;14(8):e1002533. doi: 10.1371/journal.pbio.1002533. PMID: 27541692; PMCID: PMC4991899.

[42] Labavić D, Loverdo C, Bitbol AF. Hydrodynamic flow and concentration gradients in the gut enhance neutral bacterial diversity. Proc Natl Acad Sci U S A. 2022 Jan 4;119(1):e2108671119. doi: 10.1073/pnas.2108671119. PMID: 34969835; PMCID: PMC8740595

[43] Jiang X, Hall AB, Arthur TD, Plichta DR, Covington CT, Poyet M, Crothers J, Moses PL, Tolonen AC, Vlamakis H, Alm EJ, Xavier RJ. Invertible promoters mediate bacterial phase variation, antibiotic resistance, and host adaptation in the gut. Science. 2019 Jan 11;363(6423):181-187. doi: 10.1126/science.aau5238. PMID: 30630933; PMCID: PMC6543533.

[44] Wang RJ, Al-Saffar SI, Rogers J, Hahn MW. Human generation times across the past 250,000 years. Sci Adv. 2023 Jan 6;9(1):eabm7047. doi: 10.1126/sciadv.abm7047. Epub 2023 Jan 6. PMID: 36608127; PMCID: PMC9821931.

[45] Yang Z. PAML 4: phylogenetic analysis by maximum likelihood. Mol Biol Evol. 2007 Aug;24(8):1586-91. doi: 10.1093/molbev/msm088. Epub 2007 May 4. PMID: 17483113.

[46] Ghosh OM, Good BH. Emergent evolutionary forces in spatial models of luminal growth and their application to the human gut microbiota. Proc Natl Acad Sci U S A. 2022 Jul 12;119(28):e2114931119. doi: 10.1073/pnas.2114931119. Epub 2022 Jul 5. PMID: 35787046; PMCID: PMC9282425.

[47] Lieberman TD. 2022 Detecting bacterial adaptation within individual microbiomes Phil. Trans. R. Soc. B 377 2021 024320210243

[48] Cvijović I, Good BH, Jerison ER, Desai MM. Fate of a mutation in a fluctuating environment. Proc Natl Acad Sci U S A. 2015 Sep 8;112(36):E5021-8. doi: 10.1073/pnas.1505406112. Epub 2015 Aug 24. PMID: 26305937; PMCID: PMC4568713.

[49] Feder AF, Kline C, Polacino P, Cottrell M, Kashuba ADM, Keele BF, Hu SL, Petrov DA, Pennings PS, Ambrose Z. A spatio-temporal assessment of simian/human immunodeficiency virus (SHIV) evolution reveals a highly dynamic process within the host. PLoS Pathog. 2017 May 25;13(5):e1006358. doi: 10.1371/journal.ppat.1006358. PMID: 28542550; PMCID: PMC5444849.

[50] Druelle V, Neher RA. Reversions to consensus are positively selected in HIV-1 and bias substitution rate estimates. Virus Evol. 2022 Dec 15;9(1):veac118. doi: 10.1093/ve/veac118. PMID: 36632482; PMCID: PMC9829961.
[51] Castillo-Ramírez S, Harris SR, Holden MT, He M, Parkhill J, Bentley SD, Feil EJ. The impact of recombination on dN/dS within recently emerged bacterial clones. PLoS Pathog. 2011 Jul;7(7):e1002129. doi: 10.1371/journal.ppat.1002129. Epub 2011 Jul 14. PMID: 21779170; PMCID: PMC3136474.
[52] Cooper VS, Lenski RE. The population genetics of ecological specialization in evolving Escherichia coli populations. Nature. 2000 Oct 12;407(6805):736-9. doi: 10.1038/35037572. PMID: 11048718.
[53] Vigué L, Tenaillon O. Predicting the effect of mutations to investigate recent events of selection across 60,472 *Escherichia coli* strains. Proc Natl Acad Sci U S A. 2023 Aug;120(31):e2304177120. doi: 10.1073/pnas.2304177120. Epub 2023 Jul 24. PMID: 37487088; PMCID: PMC10401003.
[54] Tataru P, Simonsen M, Bataillon T, Hobolth A. Statistical Inference in the Wright-Fisher Model Using Allele Frequency Data. Syst Biol. 2017 Jan 1;66(1):e30-e46. doi: 10.1093/sysbio/syw056. PMID: 28173553; PMCID: PMC5837693.
[55] Desai MM, Fisher DS. Beneficial mutation selection balance and the effect of linkage on positive selection. Genetics. 2007 Jul;176(3):1759-98. doi: 10.1534/genetics.106.067678. Epub 2007 May 4. PMID: 17483432; PMCID: PMC1931526.
[56] Haldane J.B.S. 1927 The mathematical theory of natural and artificial selection. Proc. Camb. Philos. Soc 23, 838–844

Acknowledgements

The authors thank all members of the Lieberman Lab for their thoughtful feedback on this manuscript. We also thank William Shoemaker for making the data used in this work easily accessible and his feedback on the manuscript. This work was funded by a grant from the National Institutes of Health (1DP2GM140922-01 to T.D.L.) and a fellowship for the National Sciences Foundation (to P.A.T.).

Code Availability

Code available at Github repository https://github.com/PaulTorrillo/Microbiome_Reversions.

Methods

Wright Fisher Simulations

The majority of the computational simulations performed are built upon the idea of the Wright-Fisher Model with selection [54]. However, we have made some changes to generalize this model for our purposes.

First, the simulations do not necessarily assume a constant population size, but rather assume the population grows via a logistic growth model with a capacity. Specifically, if P_i is the population on the ith generation and K is the population capacity, then

$$\overline{P_{i+1}} = P_i + P_i(1 - \frac{P_i}{K})$$

And

$$P_{i+1} = Poiss(\overline{P_{i+1}})$$

The population size is a Poisson random variable as we choose to determine the offspring of individual genetic classes as a Poisson random variable.

To speed the simulation up and enable simulation of very large population sizes, we implemented the Fisher-Wright model using a variety of mutational classes, rather than tracking each genotype individually. Mutational classes are somewhat different from the practice of simulating fitness classes [55]. Mutational classes can be considered as defined as a combination of fitness classes and maintained through Poisson splitting and merging. We first break the total population, P_i, at generation i into different classes. The number of individuals in class j on generation i will be A_{ij}. We have

$$P_i = \sum_{j \geq 0} A_{ij}$$

Within class j we can store a number of variables that provide information about the genotype of members of A_{ij}. Specifically, we can store a number j_k that specifies the number of mutations of type k in the class j_k. Examples of potential types that could be used include deleterious mutations, beneficial mutations, or mutations that resulted from a reversion. Each type of mutation will be associated with a specific selective advantage s_k.We can now write a formula to calculate the absolute fitness F_j of class j

$$F_j = \prod_{k \geq 0} (1 + s_k)^{j_k}$$

From the absolute fitness F_j, we calculate the average absolute fitness of the population on generation i via

$$E[F]_i = \frac{\sum_{j\geq 0} F_j A_{ij}}{P_i}$$

This allows us in turn to calculate the relative fitness of class j on generation i which will be given as

$$f_{ij} = \frac{F_j}{E[F]_i}$$

Now we can calculate the expected size of class j in the next generation with

$$A_{(i+1)j} = f_{ij}(A_{ij} + A_{ij}(1 - \frac{P_i}{K}))$$

Note that

$$P_{i+1} = \sum_{j\geq 0} A_{(i+1)j} = \sum_{j\geq 0} f_{ij}(A_{ij} + A_{ij}(1 - \frac{P_i}{K})) = \sum_{j\geq 0} \frac{F_j}{E[F]_i}(A_{ij} + A_{ij}(1 - \frac{P_i}{K})) = P_i + P_i(1 - \frac{P_i}{K})$$

This allows us to use a logistic model of growth to represent population size rather than being constrained to fixing it. This is useful for simulating bottlenecks. However, the simulation as laid out does not take into account genetic drift through random fluctuations. To do this, we rewrite the above equations to be

$$A_{(i+1)j} = Poiss(f_{ij}(A_{ij} + A_{ij}(1 - \frac{P_i}{K})))$$

Which also implies

$$P_{i+1} = Poiss(P_i + P_i(1 - \frac{P_i}{K}))$$

Note that this simulation still has equivalent dynamics of the frequencies of classes as a Wright-Fisher Model with selection in the case of a fixed population size. This is because of the ability to split Poisson processes i.e.

$$Pr(A_{(i+1)j} = X \mid P_{i+1}) = Pr(Bin(P_{i+1}, \frac{f_{ij}A_{ij}}{P_i}) = X)$$

Mutations are added in every generation depending on the mutation rate. Only single mutants are generated per generation and an organism cannot get more than one mutation per generation. The number of new mutants are determined by the binomial distribution. New mutants are added then to their appropriate class j. For example, if a deleterious mutation is gained in a class with 10 deleterious mutations (and nothing else), this new mutant will increase

the population size of the class with 11 deleterious mutations (and nothing else). By grouping individuals in classes rather than by genotype, computational cost can be greatly cut down on. Grouping individuals does not affect the dynamics of the simulation because the merging of Poisson processes is still Poisson. The downside to this approach is information loss, however in our situation we have already defined the classes to contain all the information we are interested in already.

Parameter Estimation

Data was obtained from Shoemaker and Garud [16] and was initially generated by Garud & Good et al [14]. Pairwise d_N/d_S values can be found in the Github repository. The parameters are estimated by using scipy.optimize.curve_fit. The fit minimizes the RMSD of the *logarithmic* d_N/d_S. If we fit the data by minimizing just d_N/d_S on a linear scale, we get $s \approx 2.0 \times 10^{-5}$ which suggests even weaker purifying selection (Fig. S1).

Testing Standard d_N/d_S Software

We use PAML [45] version 4.8 in order to calculate d_N/d_S on a simulated tree that ends in ten lineages. An average of 10 simulated trees is calculated for a given distance from the MRCA. The actual d_N/d_S assumes all mutations can be seen along the simulated tree. The observed d_N/d_S assumes the only nonneutral nonsynonymous (90% of nonsynonymous) mutations can be seen if they occurred within the last 100,000 generations. The actual d_N/d_S is the same tree but with all mutations visible.

Supporting Information

1.1 d_N/d_S Theory

The following is meant to provide a more indepth walkthrough of how one can build up and interpret the purifying selection model and its effect of time dependence on d_N/d_S. Assume an infinite population of organisms. Consider the existence of m classes of nonsynonymous mutations. The number of mutations of the ith class in the population is represented by the variable N_i. Each class N_i has an associated mutation rate μ_i (mutations per genome per generation per unit time) and an associated selective disadvantage s_i (mutation purification per unit time). In the purifying selection model we assume that $s_0 = 0$ and $s_{i>0} > 0$. We assume that both the mutation rate and the selective disadvantage of each class remain constant throughout time. We assume this is the global population and hence no migration. We then have

$$dN_i = \mu_i dt - s_i N_i dt \quad \text{(S1)}$$

Assuming $i > 0$, we can integrate

$$\frac{dN_i}{\mu_i - s_i N_i} = dt$$

Using u substitution, we let $u = \mu_i - s_i N_i$ so that $\frac{du}{dN_i} = - s_i$ which implies $dN_i = \frac{du}{-s_i}$ so that

$$\frac{du}{-s_i u} = dt$$

Integrating both sides we get

$$\frac{-ln(u)}{s_i} = t + C$$

Where C is the constant of integration. Continuing we have

$$u = e^{-s_i t - s_i C}$$

$$\mu_i - s_i N_i = e^{-s_i t - s_i C}$$

$$N_i = \frac{\mu_i}{s_i} - \frac{e^{-s_i t - s_i C}}{s_i}$$

We can remove the constant of integration and instead replace it by initial condition $N_i(0)$

$$N_i(0) = \frac{\mu_i}{s_i} - \frac{e^{-s_i C}}{s_i}$$

So then we have that

$$C = \frac{ln(\mu_i - s_i N_i(0))}{-s_i}$$

So that we get

$$N_i = \frac{\mu_i}{s_i}(1 - e^{-s_i t}) + N_i(0)e^{-s_i t}$$

Since $N_i(0)$ should occur at a homogenous population that is the most recent common ancestor of the individuals in the population we are observing, we assume $N_i(0)$=0 so we have

$$N_i = \frac{\mu_i}{s_i}(1 - e^{-s_i t}) \quad \text{(S2)}$$

If $i = 0$, we have

$$N_0 = \mu_0 t$$

We also assume that there are synonymous mutations S which are neutral and occur with new mutations per unit time μ_S so that

$$S = \mu_S t$$

So if we want to find N (the total number of nonsynonymous mutations), that will be given by

$$N = \mu_0 t + \sum_{i \geq 1} \frac{\mu_i}{s_i}(1 - e^{-s_i t}) \quad \text{(S3)}$$

Now observe the following with G as the number of base paris in the core genome, then d_N=$2N/(G \times 3/4)$ and d_S=$2S/(G \times 1/4)$. The two comes from the fact that there are two diverged lineages when calculating d_N/d_S

$$\frac{d_N}{d_S} = \frac{1}{3}\frac{N/G}{S/G} = \frac{\mu_0 t + \sum_{i \geq 1} \frac{\mu_i}{s_i}(1 - e^{-s_i t})}{\mu_S t} = \frac{1}{3}\left(\frac{\mu_0}{\mu_S} + \sum_{i \geq 1} \frac{\mu_i/\mu_S}{s_i t}(1 - e^{-s_i t})\right) \text{(S4)}$$

The ⅓ is for normalization. While the above form is easier to analyze in terms of actual time, it should also be noted that data is given in terms of d_S rather than t so the following equivalent form can also be helpful when discussing fitting of the timescale dependence of d_N/d_S

$$\frac{d_N}{d_S} = \frac{1}{3}\left(\frac{\mu_0}{\mu_S} + \sum_{i\geq 1} \frac{2\mu_i}{Gs_i d_S}\left(1 - e^{-\frac{Gs_i}{2\mu_S} d_S}\right)\right)$$

Furthermore, we can rewrite $\mu_i = 3\alpha_i \mu_S$ so that we have

$$\frac{d_N}{d_S} = \alpha_0 + \sum_{i\geq 1} \frac{2\alpha_i \mu_S}{Gs_i d_S}\left(1 - e^{-\frac{Gs_i}{2\mu_S} d_S}\right)$$

Which then allows us to simply rewrite $\beta_i = \frac{Gs_i}{2\mu_S}$ so that we have

$$\frac{d_N}{d_S} = \alpha_0 + \sum_{i\geq 1} \frac{\alpha_i}{\beta_i d_S}\left(1 - e^{-\beta_i d_S}\right) \qquad \text{(S5)}$$

To begin analyzing (S5), we consider the asymptotic behavior. First, we note that

$$\lim_{dS \to +\infty} \alpha_0 + \sum_{i\geq 1} \frac{\alpha_i}{\beta_i d_S}\left(1 - e^{-\beta_i d_S}\right) = \alpha_0 = \frac{\mu_0}{\mu_S} \qquad \text{(S6)}$$

For initial behavior, we can use L'Hopital's Rule

$$\lim_{dS \to +0} \alpha_0 + \sum_{i\geq 1} \frac{\alpha_i}{\beta_i dS}\left(1 - e^{-\beta_i dS}\right) = \alpha_0 + \sum_{i\geq 1} \alpha_i = \frac{\mu_0 + \sum_{i\geq 1} \mu_i}{\mu_S} \qquad \text{(S7)}$$

Finally, we are interested in when d_N/d_S ends up being in between these initial and final values. Each class i has a different midpoint at which its contribution to d_N/d_S is a half. In mathematical terms, this can be summarized as

$$\frac{\alpha_i}{2} = \frac{\alpha_i}{\beta_i d_S}\left(1 - e^{-\beta_i d_S}\right)$$

Which implies

$$\frac{\beta_i d_S}{2} = \left(1 - e^{-\beta_i d_S}\right)$$

Assuming $\beta_i d_S \neq 0$, the solution is given by the principal branch of the Lambert W function. We make the substitution $\beta_i d_S = u + 2$ so that we can rewrite the above in Lambert form

$$e^u u = \frac{-2}{e^2}$$

$u = -2$ is a solution but implies $\beta_i d_S = 0$ trivially. The other solution is the principal branch of the Lambert W function $W_0(\frac{-2}{e^2})$. For values of x close to zero, $W_0(x) \approx x$. Thus we have $u = \frac{-2}{e^2}$ and hence

$$\beta_i d_S = 2(1 - e^{-2})$$

$$d_S = \frac{2(1-e^{-2})}{\beta_i} = \frac{4\mu_S(1-e^{-2})}{Gs_i} \quad \text{(S8)}$$

Thus, we see that for any class of mutation, s_i will determine the midpoint (assuming some constant μ_S and G).

This provides the analysis of a general model, but attempting to model multiple mutation classes with different selective coefficients can be overly complex. Instead, we can use the harmonic average selective coefficient s for $i > 0$ and the nonneutral nonsynonymous mutation rate μ_N. These two variables are defined to be

$$\mu_N = \sum_{i \geq 1} \mu_i$$

And

$$s^{-1} = \sum_{i \geq 1} \frac{\mu_i}{\mu_N s_i}$$

This simplified model should work generally well. First, the initial behavior and the asymptotic behavior do not change. The midpoint is now given at

$$d_S = \frac{4\mu_S(1-e^{-2})}{Gs}$$

Which is the average midpoint of the generalized model (assuming each class contributes a midpoint proportional to the mutation range).

Taking this all into account, here is exactly what is being fit in the d_N/d_S curve. We are fitting the equation

$$\frac{d_N}{d_S} = \alpha + \frac{1-\alpha}{\beta d_S}(1 - e^{-\beta d_S}) \quad \text{(S10)}$$

α is the fraction of nonsynonymous mutations that are neutral. Now β is a compound parameter and we are able to fit $\beta = \frac{Gs}{2\mu_S}$ which is essentially half of the harmonic average of

selective disadvantages in ratio with the synonymous mutation rate per site per generation. Now we can estimate the synonymous mutation per site per generation with the following

$$10^{-9}\,\frac{mutations}{base\ pair \times generation} \times 3\,\frac{base\ pairs}{site} \times \frac{1}{4}\,\frac{synonymous\ mutation}{mutations} = \frac{3}{4} \times 10^{-9} \times \frac{synonymous\ mutations}{site \times generation}$$

Thus we are truly fitting:

$$\frac{d_N}{d_S} = \alpha + \frac{\frac{3}{4}\times(1-\alpha)\times 10^{-9}}{2sd_S}\left(1 - e^{-\frac{s}{\frac{3}{2}\times 10^{-9}}d_S}\right) \quad \text{(S11)}$$

1.2 Mutation Accumulation

In order to analyze genetic drift and Muller's Ratchet, we will provide a brief overview of the approach well suited for our work. For any nonsynonymous mutation class N_i with $i > 0$, we can track the size of a population with 0 mutations of class N_i, denoted by variable W_i, via

$$dW_i = s_i N_i(t) W_i dt - \mu_i W_i dt \quad \text{(S12)}$$

Here $N_i(t)$ is the average number of mutations of class N_i in the population. This equation reflects how every unit time, the mutation free class should increase by its selective advantage relative to the population though also lose members of the population to the mutation rate.

If we substitute in $N_i(t)$ we get

$$dW_i = s_i \frac{\mu_i}{s_i}(1 - e^{-s_i t})dt - \mu_i W_i dt$$

$$dW_i = \mu_i(1 - e^{-s_i t})W_i dt - \mu_i W_i dt$$

$$dW_i = -\mu_i e^{-s_i t} W_i dt$$

So then

$$ln(W_i) = \frac{\mu_i}{s_i} e^{-s_i t} + C$$

Assuming that W_i at time 0 is given by W_0 (representing the initial population size which under our assumptions is always free of mutations and hence wild type) then

$$ln(W_0) = \frac{\mu_i}{s_i} + C$$

$$C = ln(W_0) - \frac{\mu_i}{s_i}$$

$$W_i(t) = W_0 e^{-\frac{\mu_i(1-e^{-s_i t})}{s_i}} \quad \text{(S13)}$$

We see that if we set $W_0 = 1$, then everything can be given in terms of frequencies within the population. Asymptotically, we have that

$$\lim_{t \to \infty} W_0 e^{-\frac{\mu_i(1-e^{-s_i t})}{s_i}} = W_0 e^{-\frac{\mu_i}{s_i}} \quad \text{(S14)}$$

Importantly, we also note the following: Let W be the frequency of the wild type (mutation free class) and $W_0 = 1$. Then

$$W(t) = \prod_{i>0} W_i(t) = e^{-\sum_{i>0} \frac{\mu_i(1-e^{-s_i t})}{s_i}} \quad \text{(S15)}$$

Which implies

$$\lim_{t \to \infty} e^{-\sum_{i>0} \frac{\mu_i(1-e^{-s_i t})}{s_i}} = e^{-\sum_{i>0} \frac{\mu_i}{s_i}} = e^{-\frac{\mu_N}{s}} \quad \text{(S16)}$$

Once again using

$$\mu_N = \sum_{i \geq 1} \mu_i$$

And

$$s^{-1} = \sum_{i \geq 1} \frac{\mu_i}{\mu_N s_i}$$

Furthermore, the average time for the frequency in the population without mutations of class i to reach one half of the logarithm of the asymptotic frequency is the same when using the above simplifications. In other words, the difference in how much and how fast the wild type is lost should not really depend on the distribution of selective coefficients.

Finally, we can predict if the least loaded class will actually be lost to drift. We can form this prediction via the following. We make the assumption that if the least loaded class W drops below its steady state frequency, $e^{-\frac{\mu_N}{s}}$, it will have advantage s every generation. Any individual

with advantage s has $2s$ probability of extinction (see SI Text 2.1). If we expect there to be $N_e e^{-\frac{\mu_N}{s}}$ individuals, we can estimate that mutation accumulation will occur when

$$2sN_e e^{-\frac{\mu_N}{s}} << 1 \text{ (S18).}$$

2.1. Extinction and Fixation Probability

Here we will derive how the fixation probability of a mutation with selective advantage s is approximately $2s$. This is a standard result that can be found in classic population genetics textbooks. It is usually derived via differential equations but can also be obtained more classically from the study of branching processes [56] which we will use here. First, we assume that individuals reproduce via a Galton-Watson branching process with mean 1+s. We also assume there are no other mutations in the population that can interfere with fixation or extinction. A fundamental result from the study of branching processes is that the extinction probability is given by the smallest nonnegative root of the branching processes corresponding probability generating function, f(z). Being a Galton-Watson branching process, the probability generating function is the the probability generating function of a Poisson process so

$$f(z) = e^{(1+s)(1-z)}$$

Thus we need to find the smallest nonnegative solution, z, to

$$e^{(1+s)(1-z)} - z = 0$$

We can use a second order Taylor approximation to approximate the exponential so we have

$$1 + (1 + s)(z - 1) + \frac{((1+s)(z-1))^2}{2} - z = 0$$

Which has a smallest nonnegative solution of

$$z = \frac{s^2+1}{(s+1)^2}$$

If s is small then we have

$$z \approx \frac{1}{1+2s}$$

Which we can further approximate by doing

$$z \approx \frac{1}{1+2s}\frac{1-2s}{1-2s} \approx 1 - 2s \quad \text{(S17)}$$

If $1 - 2s$ is the extinction probability then the fixation probability will be 2s.

2.2. Accessibility of Mutations

We calculate time for mutations to occur and fix in the population for demonstration in Figure 3b. For the sake of simplicity, we consider the weak-mutation strong selection regime (no clonal interference). While clonal interference will slow the rate of any given reversion reaching fixation, it will only minorly change the frequency of a revertant with high *s* in the population, as multiple backgrounds will find the same reversion when N is sufficiently high. The expected time to fixation given a mutation with selective coefficient s is estimated using

$$(1 + s)^t = N_e$$

Where N_e is the census population size. The above implies

$$t ln(1 + s) = ln(N_e)$$

And if s is small then we have

$$t = \frac{ln(N_e)}{s} \quad \text{(S19)}$$

Now we need to know the expected time for a fixing mutant to arise. First, we want the probability the mutation arises and fixes which will be given by

$$1 - (1 - 2s\mu_{ben})^{N_e} \approx 2N_e s\mu_{ben}$$

Which implies the expected time to arisal is approximately

$$\frac{1}{2N_e s\mu_{ben}} \quad \text{(S20)}$$

So therefore we say a mutation is accessible if

$$\frac{1}{2N_e s\mu_{ben}} < \frac{ln(N_e)}{s}$$

Or alternatively written as

$$1 < 2N_e\mu_{ben} ln(N_e) \quad \text{(S21)}$$

Finally, note that the expected time to fixation is given by

$$\frac{1}{2N_e s\mu_{ben}} + \frac{ln(N_e)}{s} \quad \text{(S22)}$$

3.1 Reversion Model with Fluctuating Loci

The following is how to obtain the reversion model with fluctuating loci going from the general model. Similar to the original purifying selection model, it is possible to assume a variety of classes of mutations but for simplicity we only assume 1. If we make the following definitions for

$$R_{in} = \frac{1}{T_{adapt}}$$

$$P_{out} = \frac{2}{n_{loci} T_{adapt}}$$

we can link Equation (7) to a fluctuating loci model via

$$\frac{dN_{nonneut}}{dt} = R_{in} - P_{out} N_{nonneut} = \frac{1}{T_{adapt}} - \frac{2}{n_{pressures} T_{adapt}} N_{nonneut}$$

$$= \frac{1}{n_{loci} T_{adapt}} (n_{loci} - N_{nonneut}) - \frac{1}{n_{loci} T_{adapt}} N_{nonneut} \qquad \text{(S23)}$$

S23 can be more directly linked to a fluctuating loci model as we see the rate of nonsynonymous mutations in is proportional to $n_{loci} - N_{nonneut}$ (the number of loci unmutated) and the rate out is proportional to $N_{nonneut}$ the number of loci mutated.

Similar to the purifying selection model we have

$$N_{nonneut}(t) = \frac{n_{loci}}{2} (1 - e^{-\frac{2t}{n_{loci} T_{adapt}}}) \qquad \text{(S24)}$$

Here T_{adapt} representing the average number of generations it takes for *any* selective pressure on a loci to switch direction, and n_{loci}, the number of loci under fluctuating selective pressures. This can then be used to obtain a d_N/d_S

$$\frac{d_N}{d_S} = \frac{1}{3} \left(\frac{\mu_0}{\mu_S} + \frac{n_{loci}}{2\mu_S t} (1 - e^{-\frac{2t}{n_{loci} T_{adapt}}})\right)$$

And then

$$\frac{d_N}{d_S} = \frac{1}{3} \left(\frac{\mu_0}{\mu_S} + \frac{n_{loci}}{GdS} (1 - e^{-\frac{Gd_S}{\mu_S n_{loci} T_{adapt}}})\right)$$

If we set $\alpha = \frac{\mu_0}{3\mu_S}$, $\beta = \frac{G}{\mu_S n_{loci} T_{adapt}}$, and $\gamma = \frac{1}{3\mu_S T_{adapt}}$ so that

$$\frac{d_N}{d_S} = \alpha + \frac{\gamma}{\beta dS} (1 - e^{-\beta d_S}) \qquad \text{(S25)}$$

Which is equivalent to S10 with one more free parameter.

3.2 Implied Amounts of Superspreading

In the adapt or die (periodic selection) model, there are two potential issues: genetic drift and required levels of superspreading. The issue of genetic drift is very similar to that of the continuous purifying selection. The upside of the periodic selection model is adaptation is compatible. The downside is there needs to be superspreading. We can estimate how much superspreading takes place assuming the mutation selection balance is near equilibrium.

$$(1 + s)^{\theta \frac{\mu\Delta}{s}} \qquad \text{(S26)}$$

Where s is the averaged selective disadvantage per generation, μ is the nonneutral nonsynonymous accumulation rate per generation, Δ is the average number of generations between transmission, and θ is the proportion of the d_N/d_S to be explained. μ and s can be parametrized using the same values from fitting the continuous selection model, so $s = 3.5 \times 10^{-5}$ and $\mu = 1.01 \times 10^{-3}$. If use $\Delta = 10000$ and attempt to fully explain the decay, $(\theta = 1)$, we get expected superspreading events of 36000 transmissions. Alternatively, if we wanted to explain only 40% of the decay, we could do this while only demanding superspreading events of 66 transmissions.

SI Figures

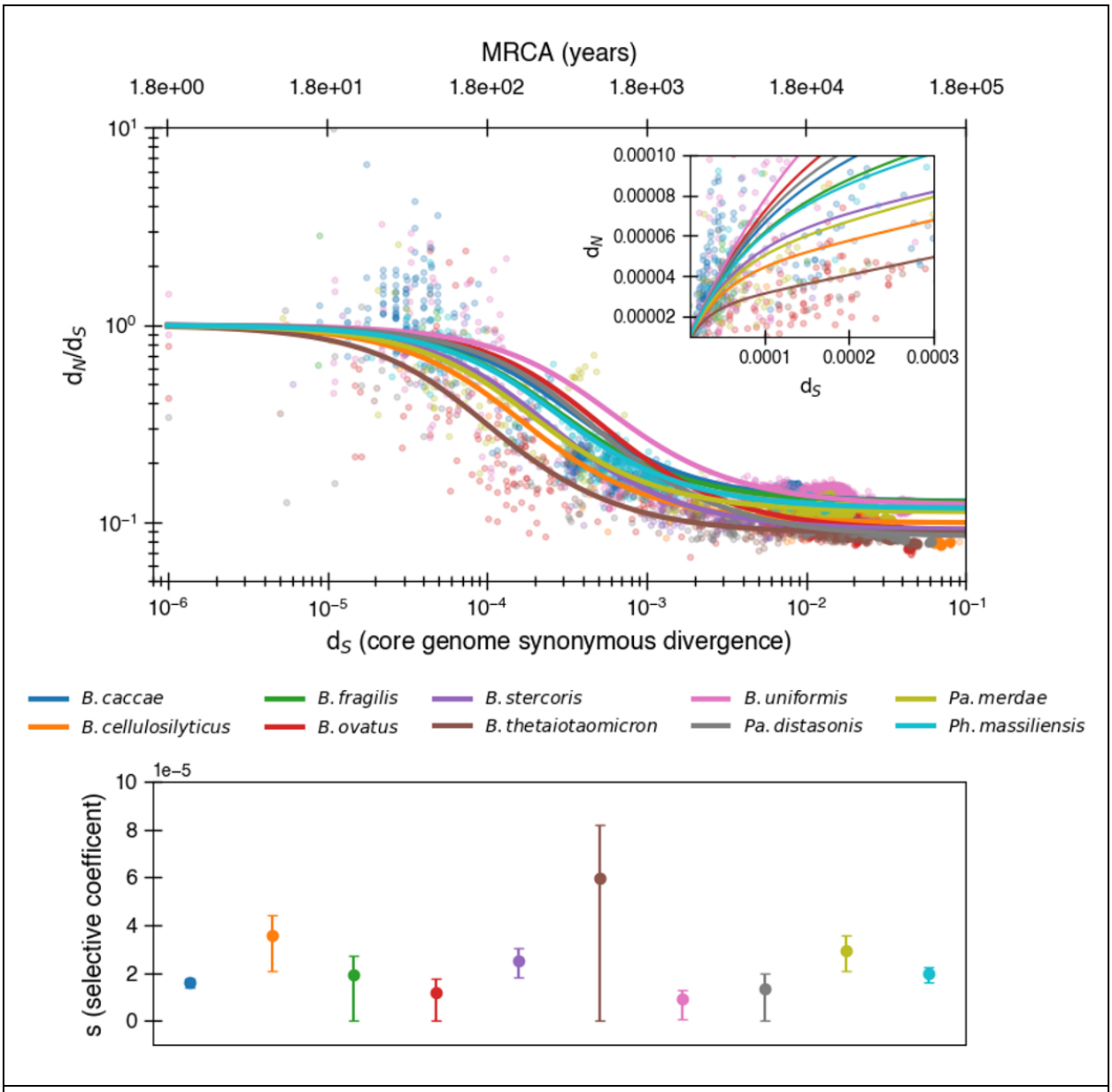

Figure S1: Purifying selection model predicts even weaker purifying selection when fitting to non logarithmic d_N/d_S: Equivalent to main text Fig. 1 except now fit is determined by minimizing variance in d_N/d_S rather than logarithmic d_N/d_S. Consequently, s values tend to be even smaller with a median of 2.0×10^{-5}. The median R^2=0.64 (range 0.07-0.88).

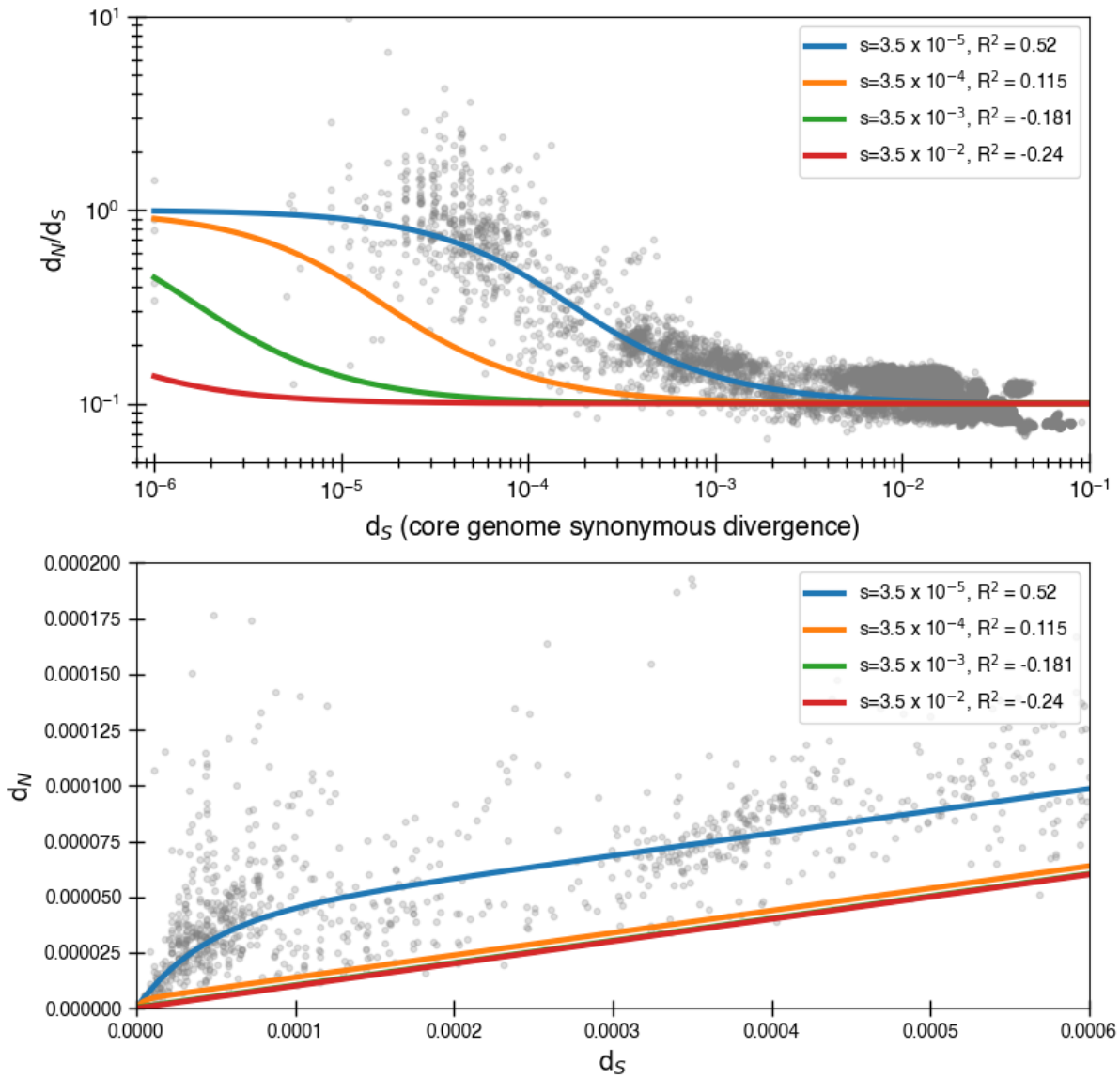

Figure S2: Larger selective coefficients rapidly lose explanatory power: Significantly larger, though still relatively small, levels of purifying selection have essentially no ability to explain the data.

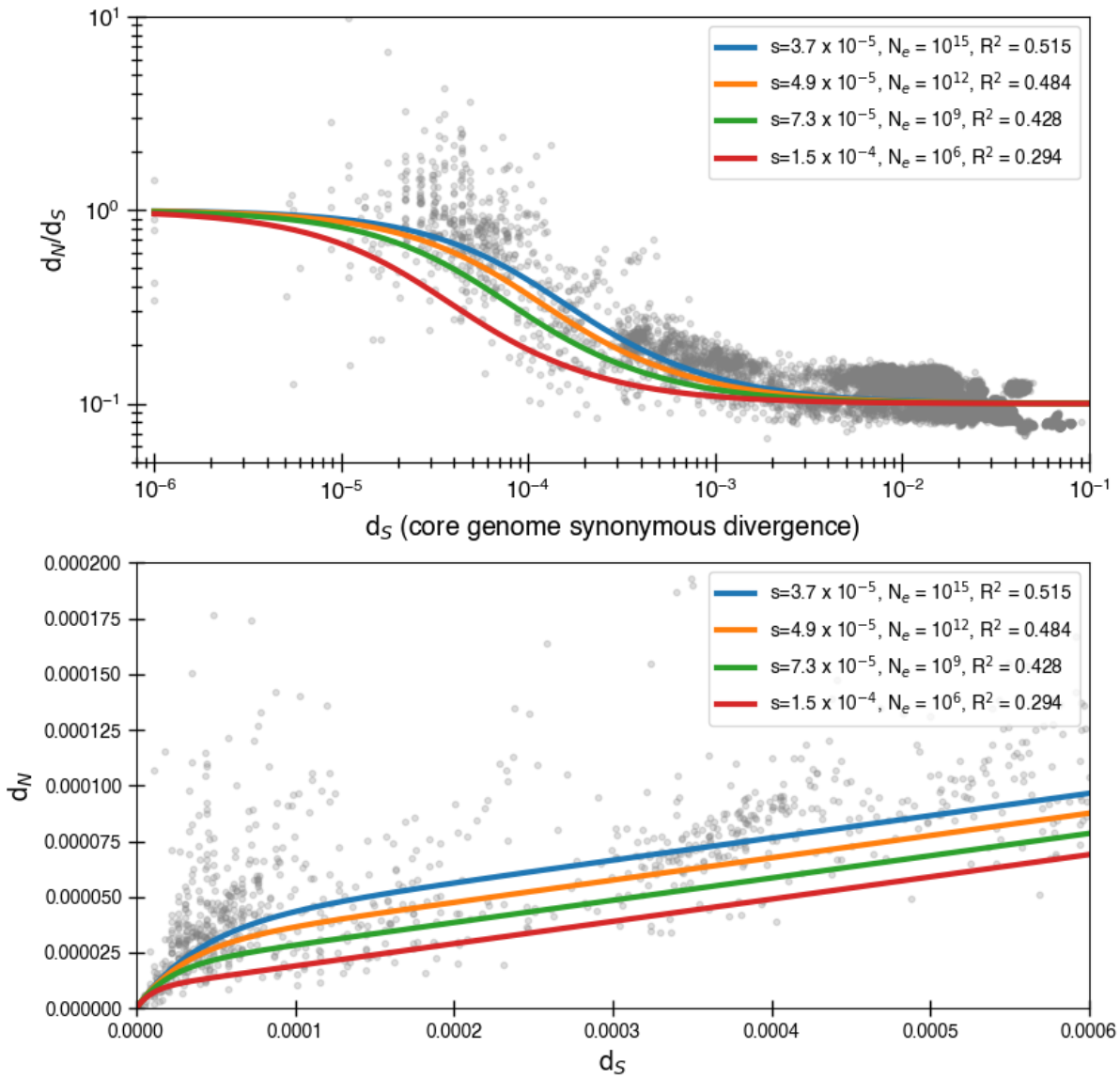

Figure S3: **Some larger selective coefficients can prevent mutation accumulation but can lead to less optimal data fit:** Displays the smallest possible s values (as estimated from S18) that should not lead to mutation accumulation for a given effective population size and the corresponding fits. The core genome size is assumed to be 1,500,000 nucleotides.

1069

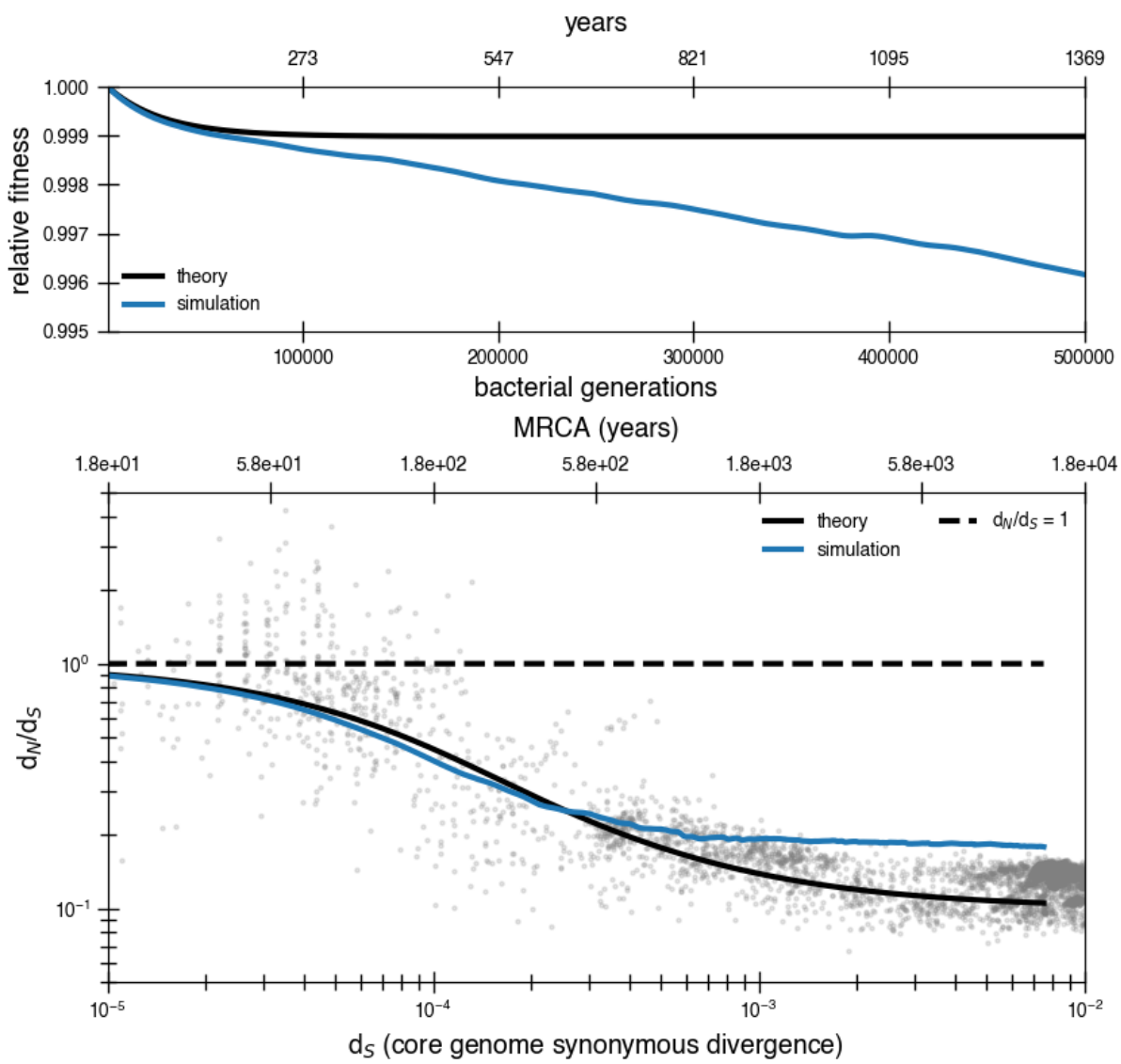

Figure S4: Even assuming all mutations are deleterious suggests a higher asymptotic d_N/d_S: A purifying selection selection simulation where all mutations are assumed to be weakly deleterious ($s = 3.5 \times 10^{-5}$). With an effective population size of 10^9 mutations still occur so quickly as to raise the asymptote above the data. Furthermore, all of these mutations contributing to the asymptotic d_N/d_S are deleterious rather than neutral.

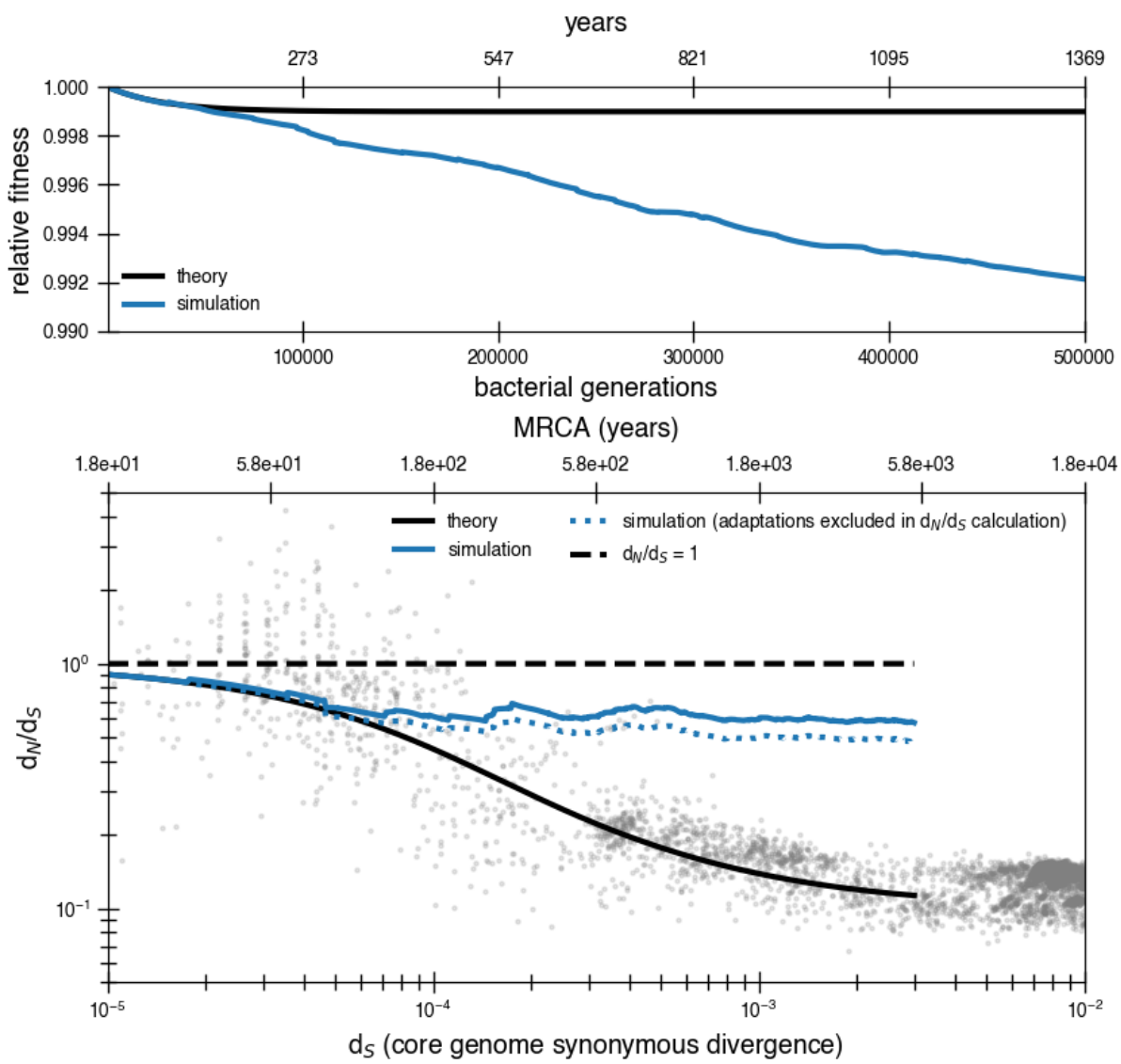

Figure S5: **Explicit transmission bottlenecks and adaptation further complicate purifying selection:** Results of a simulation with purifying selection that take into account transmission bottlenecks and the possibility of adaptation. The simulation is meant to represent a potential transmission chain from gut to gut. The census size in an individual gut is 10^{10}. Transmission bottlenecks happen on average every 100,000 generations (this is likely an underestimate but still problematic for the fit). The population is bottlenecked to 1000 members upon transmission. Beneficial mutations are released on average every 8400 generations. Multiple beneficial mutations can occur together (the number released at a time is a Poisson random variable of mean 1). This rate of beneficial mutation does not contribute much to d_N/d_S on its own as seen from the dotted line where adaptations are excluded in the d_N/d_S calculation. However, both of these scenarios drastically increase the rate of mutation accumulation and the asymptotic d_N/d_S. The reversion model is able to prevent this from occurring with 10 times the amount of adaptation and transmission.

1071

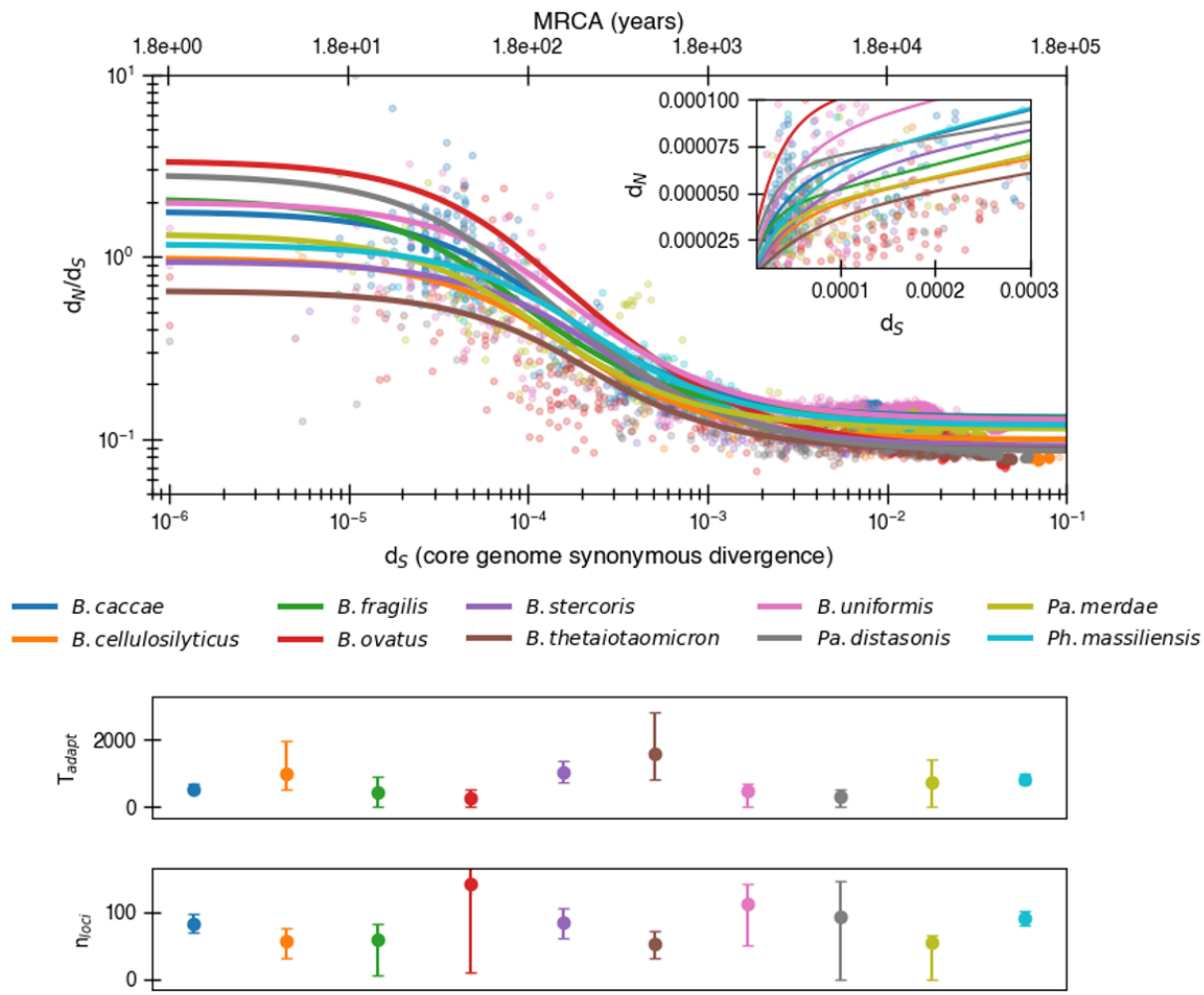

Figure S6: Potential for even more adaptation if fitting non logarithmic d_N/d_S : Results of fitting the reversion model to minimize d_N/d_S rather than logarithmic d_N/d_S. This implies potential quicker time to a switch in any selective pressure (median $T_{adapt} = 635$) and an increased number of potential loci (median $n_{loci} = 84$). The median R^2=0.72 (range: 0.11-0.88)

1072